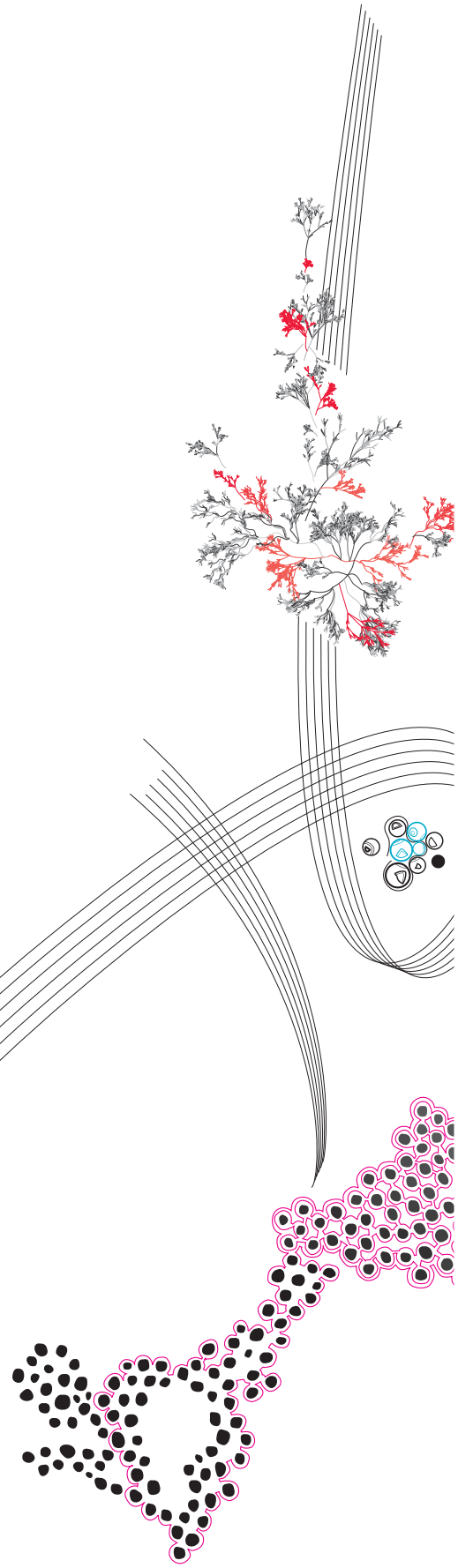

MSc Thesis Applied Mathematics

Adaptive epidemic interventions on geometric graphs

Luuk van der Werf

Supervisor: Dr. Clara Stegehuis

March, 2025

Department of Applied Mathematics
Faculty of Electrical Engineering,
Mathematics and Computer Science

UNIVERSITY OF TWENTE.

Preface

This thesis was written as final work for the Master Applied Mathematics. First of all, I want to thank dr. Clara Stegehuis for her excellent guidance over the last seven months. Without her, this would not have been possible. I want to thank dr.ing. Anne Zander and ir. Yanna Kraakman for being in my committee. Studying in Enschede for more than 6.5 years has been a great pleasure, so I want to thank everyone that contributed to that. I specifically want to thank Jorn for proofreading this thesis. Next to that, I want to thank my family for always supporting me during my studies. Lastly, I want to thank Jasmijn for her unconditional love and support.

Abstract

The COVID-19 pandemic demonstrated the need for effective intervention strategies to mitigate the spread of infectious diseases, while keeping the societal impact to a minimum. Traditional epidemic research often assumes either a homogeneous social network or fixed interventions. The assumption of homogeneous social networks ignores any geometric influence, while the assumption of fixed interventions neglects the dynamic relationship between disease prevalence and adherence to interventions. This thesis introduces a novel framework to combine adaptive intervention strategies with geometric random graphs. By introducing adaptive interventions that respond to local and global infection levels, we investigate the impact of different social distancing approaches, including distance-based, weight-based, and infection probability-based interventions. Through extensive simulations on randomly generated as well as real-life networks, we find that both targetting high-degree nodes and targetting long distance edges are effective in reducing peak and total infections. Furthermore, our results show that local information might be beneficial, by focussing interventions on the infected areas. However, the adaptive methods do not consistently outperform the threshold methods, which implies that the feedback relation between adherence to the measures and the disease prevalence does not always have a positive impact.

Keywords: Epidemic modelling, adaptive interventions, geometric random graphs, social distancing, network-based models.

Contents

1 Introduction **3**

2 Background information **5**
2.1 Compartment models . . . 5
2.1.1 SIR model . . . 5
2.1.2 SIS model . . . 5
2.1.3 SITS model . . . 6
2.1.4 Other compartment models . . . 6
2.2 Epidemics on networks . . . 7
2.3 Geometric random graphs . . . 7

3 Related work **9**

4 Model **11**
4.1 Generating GIRGs . . . 11
4.2 Modelling interventions . . . 11
4.2.1 Distance based . . . 11
4.2.2 Weight based . . . 12
4.2.3 Adaptive infection probability . . . 12
4.2.4 Random percolation . . . 12
4.2.5 Threshold models . . . 13
4.3 Imperfect information . . . 13
4.3.1 Local information . . . 13
4.3.2 Information delay . . . 14

5 Theoretical results **15**
5.1 Expected degree of GIRG . . . 15
5.2 SIS equilibrium . . . 18

6 Simulation results **20**
6.1 Key metrics . . . 20
6.2 Parameter choices . . . 22
6.3 Comparison of intervention strategies . . . 23
6.4 Effect of local information . . . 29
6.5 Effect of delay . . . 32
6.6 Adaptive compared to threshold . . . 34
6.7 Using flight data as input network . . . 37

7 Discussion **39**
7.1 Analysis of simulation results . . . 39
7.2 Comparison with existing literature . . . 40
7.3 Limitations and possible improvements . . . 40
7.4 Future research . . . 41

8 Conclusion **42**

1 Introduction

As of March 2025, the COVID-19 pandemic has claimed the lives of more than 7 million people [5]. Next to this, the pandemic and the attempts to mitigate the viral spread have caused enormous financial, physical and mental damage. The COVID-19 pandemic has demonstrated that the world was not prepared for such a virus, and a new pandemic could again be a catastrophe for healthcare and economics on a global level. This highlights the utmost importance of research aimed at understanding the spread of viruses. The COVID-19 pandemic also added a new dimension to the study of disease spread. Never before did we see so-called non-pharmaceutical interventions (NPIs) on a global scale. NPIs include a range of public health measures, primarily implemented by governments, aimed at reducing viral transmission. Examples of NPIs are lockdowns, handwashing guides, curfews, social distancing, face covering, and travel restrictions. All these intervention strategies aim to reduce the spread of the virus, but the effectiveness of some of these interventions has been questioned. Since some of these interventions can have a huge societal impact, it is important to examine their effectiveness.

Multiple papers have investigated the influence and effectiveness of interventions on epidemic spread using mathematical models [9, 10, 13, 16, 20]. In epidemiology, mobility and geographic locations are important components, which can change the course of the epidemic. Especially when considering interventions that influence mobility, such as social distancing or travel restrictions. We can use the geometric networks to model the intervention strategies that rely on geometric distance between individuals. In geometric networks or graphs, vertices have a geometric position. However, most existing epidemic models are compartment models, assuming homogeneous populations and lacking a geometric structure. There are a few papers that have used network-based models which include a geometric structure to investigate the effectiveness of NPIs [14, 19, 21]. All these papers implement fixed interventions, which means they are implemented at a specific time point, and do not change over time. While this reflects the interventions taken by governmental bodies, it does not take compliance with the interventions into account. The COVID-19 pandemic demonstrated that not every individual is willing to adhere to strict interventions, and that this can seriously affect the effectiveness of these strategies. Especially when the prevalence of the infection is low, people tend to ignore certain rules [22]. This thesis introduces a new framework for modelling adaptive intervention strategies that depend on disease prevalence. To our knowledge this is one of the first studies that combines network-based models with adaptive intervention strategies. The goal of this study is to get better insight into the feedback relation between the disease prevalence and the adherence to interventions. This leads to our research question: *'How do adaptive intervention strategies on geometric random graphs influence the spread of infectious diseases?'*. This thesis conducts an extensive simulation study on the effects of the intervention strategies on different disease models, networks and model setups.

Our findings suggest that targeted intervention strategies outperform random strategies, especially those targeting high-degree nodes. Additionally, it suggests that local information can improve the mitigation of viral spread, by focussing on the infected areas. However, the adaptive intervention strategies do not significantly outperform the threshold strategies. This implies that the feedback relation between adherence to the interventions and the disease prevalence is not always beneficial.

This thesis is organised as follows: Section 2 introduces the existing models and needed background information. Section 3 reviews the scientific work related to this thesis. Section 4 explains the setup of the model, while Section 5 shows some theoretical results. Section 6 presents the results of the simulations of this model, followed by a discussion and conclusion in Sections 7 and 8, respectively.

2 Background information

In this section we will introduce the needed background information for the rest of this thesis.

2.1 Compartment models

One of the most used classes of models to predict the spread of viruses is the class of compartment models [17]. Compartment models subdivide a population into different compartments, and use differential equations to model epidemic spreading.

2.1.1 SIR model

The widely used SIR model divides a population into three classes: Susceptible, Infected and Recovered. This model was first mentioned by Kermack and McKendrick in 1927 [15]. Based on the settings and parameters of the model, population members can progress between the three compartments S, I and R. In the basic SIR model, people in the susceptible compartment S can progress to the infected compartment I, and people in the infected compartment can progress to the recovered compartment R. The classical SIR model can be described by the following ordinary differential equations (ODEs):

$$\frac{dS}{dt} = -\beta IS, \tag{1}$$

$$\frac{dI}{dt} = \beta IS - \delta I, \tag{2}$$

$$\frac{dR}{dt} = \delta I, \tag{3}$$

where S, I and R are the number of Susceptible, Infected, and Recovered/Removed individuals respectively, such that $S + I + R = N$, with N the total number of individuals in the system. Here, β is the infection rate and δ is the recovery rate. β and δ can differ greatly per disease. Based on the parameters β, δ and N, the course of the epidemic can be calculated numerically. The SIR model gives a good representation of diseases with long-lasting immunity, such as measles and hepatitis A.

2.1.2 SIS model

A well known alternative to the SIR model is the SIS model. In the SIS model individuals can recover, but move back to the Susceptible compartment, instead of to a Recovered compartment. This relates to infections for which there is no long-lasting immunity. Examples of diseases without long-term immunity are Malaria, Influenza and Gonorrhoea, and are called re-emerging diseases [2]. The rate of change for the Susceptible compartment can be described by

$$\frac{dS}{dt} = \delta I - \frac{\beta IS}{N}. \tag{4}$$

Since there are only two compartments, all individuals leaving the Susceptible compartment move into the Infected compartment, and vice versa. Therefore,

$$\frac{dI}{dt} = -\frac{dS}{dt} = -\delta I + \frac{\beta IS}{N}. \tag{5}$$

In the SIS model, diseases rarely die out completely. Instead, the epidemic will often reach an equilibrium state, in which the amount of infected and susceptible individuals stabilizes. In Section 5 we approximate the equilibrium for a SIS model on a geometric graph when interventions are applied.

2.1.3 SITS model

A combination of the SIR and SIS model is the SITS model. Instead of moving from Infected to Recovered, individuals move from Infected to the Temporary immune compartment. This compartment acts similar to the recovered compartment: individuals in this compartment cannot be infected, and cannot infect others. The only difference is that individuals can move back from the temporary immune compartment to the susceptible compartment, hence S-I-T-S. Every temporary immune individual can lose its immunity with rate η. This gives an average immune period of $\frac{1}{\eta}$. The deterministic SITS model can be described by the following ODEs:

$$\frac{dS}{dt} = -\frac{\beta IS}{N} + \eta T, \tag{6}$$
$$\frac{dI}{dt} = \frac{\beta IS}{N} - \delta I, \tag{7}$$
$$\frac{dT}{dt} = \delta I - \eta T. \tag{8}$$

2.1.4 Other compartment models

Many more variants of the previously mentioned compartment models exist. The SEIR model is for example another variant on the basic SIR model. The SEIR model introduces the Exposed compartment. Before getting infected, individuals first move to the Exposed compartment, which means they are exposed to the infection, but are not ill yet, which means they cannot transfer the infection to others. Individuals stay in the Exposed compartment for an average incubation period T_{inc}, which makes the rate for transferring from the Exposed compartment to the Infected compartment $\omega = \frac{1}{T_{inc}}$. For a homogeneous population, the SEIR model can be described by the following ODEs:

$$\frac{dS}{dt} = -\frac{\beta IS}{N}, \tag{9}$$
$$\frac{dE}{dt} = \frac{\beta IS}{N} - \omega E, \tag{10}$$
$$\frac{dI}{dt} = \omega E - \delta I, \tag{11}$$
$$\frac{dR}{dt} = \delta I. \tag{12}$$

The SEIR model is widely used in the modelling of viruses like COVID-19, since such diseases show the presence of an incubation period, which does influence the expected course of the epidemic.

Other variants have been suggested. For example, a Vaccinated compartment can be added, the SEIR and SITS model can be combined to a SEITS model, etc. The implementation of those models is relatively straightforward, but adding more compartments makes the analysis of the results much more complex. That is why this thesis will focus on relatively simple models.

2.2 Epidemics on networks

The compartment models in Section 2.1 implicitly assume a homogeneous population where all individuals interact uniformly. This makes calculation easy, but it is an unrealistic simplification. People have their own social circles, and do not have contact with the whole population. Next to this, individuals are not identical. Some individuals have a lot contacts, while others keep their contacts to a minimum. While this is an important feature of social networks, equation-based models assume that all members of a population have identical rates of disease-causing contacts. To model the inhomogeneous nature of social networks, we resort to a network-based approach.

Consider an undirected graph $G = (V, E)$, with V a set of vertices, and $E \subseteq \{(u, v) \mid u, v \in V\}$ a set of edges between vertices in V. A person in a social network corresponds to a vertex $v \in V$, and can only be infected via vertices u that are incident to v. This structure can for example also be used in the SIR model. Vertices can have one of the three statuses: Susceptible, Infected or Recovered. Every time step, infected vertices can infect susceptible neighbouring vertices with probability β. Infected vertices can recover every time step with probability δ.

Network-based models are more specific, but also are much more computationally heavy than equation-based approaches. Equation-based models can be quickly solved numerically, while the running time for network-based models increases polynomial with the population size. This is due to the fact that the equation-based models only have one equation per compartment, while network-based models would have one equation per node in the graph. Since solving a system with potentially thousands of equations is not feasible, the network based models are usually simulated multiple times, such that the average of the simulations will give a good approximation of the expected epidemic.

2.3 Geometric random graphs

To analyse the behaviour of epidemics on different networks, we use so-called *random graphs*. Random graphs are graphs whose edges are generated randomly according to specific parameters or probability distributions. Popular random graph generators include the Erdös-Réyni model [12] and the configuration model [7]. While these models have many desirable properties, they have no geometric or spatial structure. With a geometric structure we mean that the nodes in the network have a spatial position. Real-world networks often have a geometric structure, where the probability of two individuals having a connection increases if they are geometrically close. This is realistic, since people mainly have short distance connections, and only a few long distance connections. The geometric structure is needed if we want to model interventions that are based on distance, such as social distancing or travel restrictions.

A random graph model that includes geometry is the Geometric Inhomogeneous Random Graph (GIRG) model [8]. GIRGs are scale-free networks, which are networks whose degree distributions follow a power law. This means that the fraction $P(k)$ of nodes in the network having k connections is distributed as $P(k) \sim k^{-\gamma}$, with $2 < \gamma < 3$. Scale free networks have the property that the majority of the nodes have a small number of connections, while a few nodes have a very large number of connections. These nodes are sometimes called *hubs*. To generate a GIRG, we need to generate a weight w_v and a position x_v for each vertex $v \in V$. The weights will independently be sampled from a

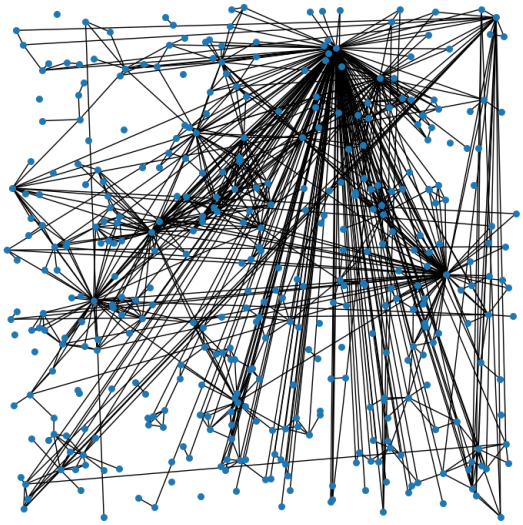

FIGURE 1: Example of a GIRG with 400 vertices and an average degree of 5.

power-law distribution with density $f(w) \sim w^{-\gamma}$, with $2 < \gamma < 3$. In general for GIRGs, we uniformly draw positions $x_v \in T^d$ for each vertex v, where T^d is the d-dimensional torus. For simplicity, this thesis will only consider positions sampled from $[0,1]^2$, for which all the properties of GIRGs stay the same. The edge probability between vertices u and v is defined as follows:

$$p_{uv} = \min\{(\frac{w_u w_v}{W||x_u - x_v||})^\alpha, 1\}, \tag{13}$$

where $\alpha \in [1, \infty)$ and $W = \sum_{v \in V} w_v$. The distance between two vertices $||x_u - x_v||$ is defined as the two dimensional euclidean distance. For $\alpha \to \infty$, we get

$$p_{uv} = \begin{cases} 0, & \text{if } \frac{w_u w_v}{W||x_u - x_v||} < 1 \\ 1, & \text{if } \frac{w_u w_v}{W||x_u - x_v||} \geq 1 \end{cases}. \tag{14}$$

From these equations we see that two things influence the edge probability between two vertices: their weights and the distance between the vertices. Higher weights result in a higher probability, and a longer distance results in a lower probability. This means that there will be relatively few long edges. Furthermore, vertices with a high weight will on average have the highest degree. In Figure 1 we see an example of a GIRG with 400 vertices.

3 Related work

Since the recent COVID-19 pandemic and its intervention strategies disrupted the lives of billions of people, an overwhelming amount of research has been conducted to model the epidemic spread and the influence of a wide range of modelling choices on the spread. Also before the COVID-19 pandemic, epidemic modelling has been a well-established research field. In this section we will give a brief overview of the various areas and focus points of recent research which relate to this work in some way.

An important factor in the realistic modelling of epidemics is accurately representing interventions. To realistically model interventions, we need to take human behaviour into account, since this influences the effectiveness of the interventions. In this thesis we try to model human behaviour by letting the prevalence directly influence the effectiveness of the interventions. Multiple other papers have included human behaviour in their models. Most of them use non-network based epidemic models, such as compartment models. Epstein et al. [11] models fear for the disease as a disease itself, with spreading mechanics that are similar to a 'normal' epidemic. Fenichel et al. [13] considers the utility between social connections and the risk of infection. Individuals in this model try to maximize their utility, which is closely related to the mathematics in economics. Saad-Roy and Traulsen [20] models the adherence to interventions using game theory. In this study, the prevalence directly influences the adherence level, which is similar to our work. In general, all these studies conclude that implementing human behaviour in epidemic models induces a feedback loop which can cause multiple infection peaks. Multiple other studies look at implementing fixed interventions, using equation-based models, but lack the focus on human behaviour [9, 10].

While Epstein et al. [11] partly looks at a agent based model, Saad-Roy and Traulsen [20] and Fenichel et al. [13] do not use an agent-based or network-based model. Like many traditional epidemiological studies, these studies are equation-based, which means they use differential equations to describe the dynamic relationships and interactions between individuals in a system at an aggregate level. Contrary to research that uses equation-based models, this thesis uses a network-based model. This means that the status of every individual in the network is tracked and calculated.

There are some other studies that look into epidemic interventions using network-based models. Jorritsma et al. [14] considers a SITS model on GIRGs. This article discusses the effect of multiple intervention strategies on the spread of viral infections. In the study, interventions are applied permanently for the entire duration of the epidemic. Syga et al. [21] considers a SEIR model on a Watts–Strogatz small-world network. They implement their interventions based on time: there are no interventions in the start, strong interventions during the peak of the epidemic, and mild interventions in the end. Marquioni et al. [16] also considers a SEIR model, on scale free networks. They also study fixed interventions, varying the start and end date. Instead of applying the interventions deterministically, it is more realistic to apply the interventions after the epidemic reaches a certain prevalence threshold. This is what done by Panicker and Sasidevan [19]. They use geometric random graphs, which can evolve by the adaptive actions and mobility of the individuals in the network. The adaptive actions are only implemented when the prevalence reaches a certain threshold. This is also what happened during the COVID-19 outbreak: only after the virus was widely spread, interventions were imposed. While applying uniform interventions

after a certain epidemic threshold is more realistic, it assumes full compliance with these measures. The COVID-19 outbreak made clear that full compliance cannot be assumed, especially when disease prevalence is low, or when the illness is perceived as mild. That is why this thesis will model interventions of which the compliance depends on the prevalence of the disease.

4 Model

We will model the epidemic spread using a time discretization. Every time step will represent a day. As explained in Section 2.2, every time step we update the disease status of the nodes in the graph. The options for this status depend on the choice of model. If the selected model is the SIR model, every node can have one of the three statuses: Susceptible, Infected, or Recovered. Every time step, infected vertices can infect susceptible neighbouring vertices with probability β. Infected vertices can recover every time step with probability δ. If the selected model is the SIS model, every node can only have the status Susceptible or Infected.

4.1 Generating GIRGs

As explained in Section 2.3, GIRGs can be created by generating weights w_v and positions x_v for every vertex $v \in V$. Based on the weights and positions, you find the edge probabilities, which can be converted in the actual graph. Since this is a tedious process, we use the GIRG generator by Bläsius et al. [6]. This generator takes the desired average degree as input, which allows us to easily select the average degree of our graph. This would otherwise depend on the choice of γ in the density function $f(w) \sim w^{-\gamma}$.

4.2 Modelling interventions

In this section we will explain in which ways we will model adaptive interventions with dependence on the disease prevalence.

4.2.1 Distance based

During the recent COVID-19 pandemic interventions limited or discouraged travelling. To analyse how this influenced the virus spread, we can use the geometric structure of GIRGs. Interventions on travel often target connections with a large distance between them. This is why as an effect of the intervention in our model, long edges will be deleted. There are multiple ways to implement this. An intuitive method is to calculate the Euclidean distance between every two nodes u, v that are connected with an edge. If this distance is bigger than a predefined threshold, which can be dependent on the prevalence, the edge will be deleted for time step t. The effectiveness of the intervention, or compliance with the intervention will be based on the prevalence I of the epidemic. For example, if the population consists of 100 individuals, and 50 of those individuals are infected, I equals $\frac{50}{100} = 0.5$. We can make the threshold dependent on the prevalence with the following algorithm. In the algorithm we introduce a parameter SDP, which stands for social-distance power. This parameter influences how effective or strict the intervention will be. If SDP is large, the interventions will be more effective or strict. In Section 6 we will discuss the influence of this parameter.

For every edge (u, v) we check if the distance $d_{uv} = ||x_u - x_v||$ exceeds the threshold. If

$$d_{uv} > \sqrt{2} \cdot (1 - I_t)^{SDP} \tag{15}$$

we delete edge (u, v) for time step t. The algorithm will be performed every time step, since the prevalence I_t can change every time step. When I is large, $(1 - I)$ will be small, which means that a lot of edges will be deleted. When $I = 0$, which means there are no

infections, no edges will be deleted, which is desired. This algorithm deletes the edges that are longer than $\sqrt{2} \cdot (1 - I)^{SDP}$. Since the vertex positions are sampled from $[0, 1]^2$, the maximum possible edge length is between u and v with $x_u = (0, 0)$ and $x_v = (1, 1)$, which gives $d_{uv} = \sqrt{2}$.

4.2.2 Weight based

Since the GIRG model assigns a weight to every vertex, we can also use this to model social distancing. Decreasing the weights w_u and w_v of vertices u and v decreases the probability of the existence of edge (u, v), so multiplying all weights with a factor between 0 and 1 will result in fewer edges. Since the prevalence I is a value between 0 and 1, we can use this as factor to scale the weights:

$$w_{v,t} = w_v \cdot (1 - I_t)^{SDP}, \ \forall v \in V, \tag{16}$$

where, $w_{v,t}$ is the weight of vertex v at time t. Again, the parameter SDP determines the strictness of the interventions. After the weights have been updated, the edges will be regenerated. This method will delete edges (u, v) that are present in the original graph when $\frac{w_u w_v}{W||x_u - x_v||} \geq 1$, and $\frac{w_{u,t} \cdot w_{v,t}}{W_t||x_u - x_v||} < 1$.

This intervention method can be realistic, since on average, it proportionally has the same impact on every individual in the network. A high weight individual might lose more connections, but also has more connections in total. This relation can be seen from Lemma 3.4 of Bringmann et al. [8]. It states that for any $v \in V$ we have $\mathbb{E}[\deg(v)] = \Theta(w_v)$. This translates to the fact that the node degrees are proportional to their weights. Since we scale all our weights with the same factor, the proportions between the node degrees will also stay the same. This means that high-degree nodes, or so-called hubs, will lose more edges on average. We will also show this in Section 5. This can be relevant, since hubs can serve as super-spreaders, which significantly accelerates disease transmission over a network.

4.2.3 Adaptive infection probability

The distance- and weight-based methods model interventions by changing the network structure. While this models the decrease of social contacts during an epidemic, it does not model interventions that try to decrease the infectiousness, such as wearing face masks, washing hands, and keeping 1.5 meter distance. To model this behaviour we will scale down the infectiousness β per time step to β_t, based on the prevalence at time t: $\beta_t = \beta \cdot (1 - I_t)$. For example, if the infection probability $\beta = 0.3$, and $I_t = 0.4$ at time t, our adjusted infection probability will be $\beta_t = \beta \cdot (1 - I_t) = 0.3 \cdot 0.6 = 0.18$. Again, we add a power SDP, to adjust the effectiveness of the interventions. This gives

$$\beta_t = \beta \cdot (1 - I_t)^{SDP}. \tag{17}$$

4.2.4 Random percolation

To compare our specific intervention models, we need a benchmark intervention strategy. For this we will use *random percolation*. Instead of deleting specific edges, we will randomly delete edges every time step t, based on the prevalence I_t. Random percolation allows us to compare structured interventions (distance and weight based) with randomly deleting edges.

We delete an edge e if

$$(\text{random}[0,\ 1])^{SDP} < I_t \tag{18}$$

where random[0, 1] is a random number uniformly sampled from the interval $[0, 1]$. This means that if $SDP = 1$, and for example $I_t = 0.5$, on average half of the edges will be deleted. If SDP is higher, more edges will be deleted. Again, if $I_t = 1$ all edges will be deleted, and if $I_t = 0$ no edges will be deleted, which is what we want.

4.2.5 Threshold models

Instead of adapting our interventions directly based on the current disease prevalence I_t, other papers, for example Panicker and Sasidevan [19], have opted to implement fixed interventions when a certain epidemic threshold is reached, and to stop the interventions when the prevalence is again below the threshold. To compare our results directly to this method, we have implemented this option in our own model. This means that we only apply our intervention methods if the threshold M is reached. If this threshold is reached, we need to specify the chosen fixed interventions. We introduce the parameter F that determines the strength of the fixed interventions. $F = 0$ leads to a complete lockdown, while $F = 1$ is equivalent to no interventions, which results in its range being $0 \leq F \leq 1$. In our intervention methods, F replaces $(1 - I)^{SDP}$.

In the distance based threshold method, we remove edge (u, v) if

$$d_{uv} > \sqrt{2} \cdot F. \tag{19}$$

In the weight based threshold method we scale the weights by F:

$$w_{v,t} = w_v \cdot F. \tag{20}$$

In the infection probability threshold method, we adjust our infection probability with a factor F:

$$\beta_t = \beta \cdot F. \tag{21}$$

In the random percolation threshold method every edge has an deletion probability of $1 - F$.

4.3 Imperfect information

4.3.1 Local information

All the aforementioned intervention methods use a global prevalence I, on which the effectiveness of the interventions depends. This assumes that all individuals in the network have access to up-to-date and correct information about the global prevalence. Even though this might be possible by (inter)national news networks, we live in an era where misinformation is widespread. People might care more about infections in their own social circles than the prevalence in the whole network. So, instead of looking at the global prevalence, we calculate the local prevalence for each individual in the network. We define the modelling option *local information* with local prevalence I_v as

$$I_v = \frac{\#\text{infected neighbours of v}}{\deg(v)},\ \forall v \in V.$$

This means that if an individual v has 5 social connections, of which 2 are infected, the observed prevalence is $I_v = 2/5 = 0.4$. Since for every node v there is a different prevalence I_v instead of global prevalence I, we need to adjust our intervention methods to this.

In the distance based algorithm we cannot immediately interchange I with I_v, since every edge is incident to two nodes, u and v. To use both I_u and I_v, we define $I_{uv} = \frac{I_u + I_v}{2}$, taking the average of I_u and I_v. We can then use this to adjust the distance based method. We delete edge (u, v) if

$$d_{uv} > \sqrt{2} \cdot (1 - I_{uv})^{SDP} \tag{22}$$

We can also use the local information for the adaptive infection probability method. To use the local information, we will adjust the infectiousness β per individual: $\beta_v = \beta \cdot I_v$. Per connection (u, v) between an infected an healthy individual, we use the average infectiousness $\beta_{uv} = \frac{\beta_v + \beta_u}{2}$ to calculate the infection probability.

The weight based method is not implemented with local information. For random percolation, local information is not applicable, since it is not based on the actions of individuals in the network.

4.3.2 Information delay

As said before, information flows are rarely perfect. Often there is a delay before information gets to people. Especially when talking about infectious diseases, there usually is a delay between the moment of infection, and the moment the virus is noticed and counted in the infection numbers. This is why we introduce the modelling option of *information delay*. If I_t is the true prevalence at time t, and we use an information delay of D time steps, our perceived prevalence at time t will be

$$I_{\text{per},t} = \begin{cases} I_{t-D} \text{ if } t \geq D \\ 0 \text{ if } t < D \end{cases} . \tag{23}$$

Information delay can be used in combination with all the mentioned intervention models, as well as in combination with local information. In Section 6.5 we will investigate if delay always has negative impact, or if some delay could have benefits.

5 Theoretical results

5.1 Expected degree of GIRG

Given a vertex with a specific weight in a GIRG, we can approximate its expected degree. Michielan et al. [18] shows that the average degree of a GIRG can be approximated as follows. Here, $p[w_i, w_j, x_i, x_j]$ is the probability of an edge between vertices i and j with their respective weights and positions. $(a \wedge b)$ is defined as the minimum of a and b. The notation $\mathbb{E}_y$ means that the averaging occurs with respect to random element y. For calculation reasons, we calculate the results in one dimension.

$$\mathbb{E}_{x_j}[p(w_i, w_j, x_i, x_j)] = 2\int_0^{\frac{1}{2}} (\frac{w_i w_j}{W||x_i - x_j||} \wedge 1)^\alpha \, dx_j$$
$$= 2\int_0^{\frac{1}{2}} (\frac{w_i w_j}{W||x_j||} \wedge 1)^\alpha \, dx_j$$

$$r_0 = \frac{w_i w_j}{W}$$

and

$$0 \leq ||x_j|| \leq \frac{1}{2},$$

so if $r_0 \geq \frac{1}{2}$ the integrand is always 1. So we look at the case when $r_0 < 1/2$:

$$\mathbb{E}_{x_i,x_j}[p(w_i, w_j, x_i, x_j)]$$
$$= 2\int_0^{r_0} (\frac{r_0}{||x_j||} \wedge 1)^\alpha dx_j + 2\int_{r_0}^{\frac{1}{2}} (\frac{r_0}{||x_j||} \wedge 1)^\alpha dx_j$$
$$= 2\int_0^{r_0} 1 \, dx_j + 2\int_{r_0}^{\frac{1}{2}} (\frac{r_0}{x_j})^\alpha dx_j$$
$$= 2(r_0 + r_0^\alpha \int_{r_0}^{\frac{1}{2}} \frac{1}{x^\alpha} dx)$$
$$= 2(r_0 + r_0^\alpha [\frac{x^{1-\alpha}}{1-\alpha}]_{r_0}^{\frac{1}{2}})$$
$$= 2(r_0 + r_0^\alpha (\frac{2^{\alpha-1} - r_0^{1-\alpha}}{1-\alpha}))$$
$$= 2r_0 + \frac{2^\alpha r_0^\alpha - 2r_0}{1-\alpha}$$
$$= r_0(2 + \frac{2}{\alpha - 1}) + O(r_0^\alpha)$$

So we conclude

$$\mathbb{E}_{x_i,x_j}[p(w_i, w_j, x_i, x_j)] = \begin{cases} 1, \text{ if } w_j \geq \frac{W}{2w_i} \\ (\frac{2w_i w_j}{W})(1 + \frac{1}{\alpha - 1}) + o(\frac{w_i w_j}{W}), \text{otherwise} \end{cases}$$

Integrating over the weight gives us

$$\mathbb{E}_{w_j}[\mathbb{E}_{x_i,x_j}[p(w_i,w_j,x_i,x_j)]]$$
$$\approx \int_1^{\frac{W}{2w_i}} (1+\frac{1}{\alpha-1})\frac{2w_i}{W} w^{-\gamma+1} dw + \int_{\frac{W}{2w_i}}^{\infty} w^{-\gamma} dw$$
$$= (1+\frac{1}{\alpha-1})\frac{2w_i}{W}(\frac{\frac{W}{2w_i}^{2-\gamma}-1}{2-\gamma}) + \frac{\frac{W}{2w_i}^{1-\gamma}}{\gamma-1}$$
$$= (1+\frac{1}{\alpha-1})\frac{2w_i}{W(\gamma-2)} + O((\frac{w_i}{n})^{\gamma-1}).$$

From this we conclude that that probability of an edge between i and any j is proportional with the weight of i, divided by the size of the network n. Since this probability is between i and the other $n-1$ vertices, our expected degree is proportional to weight w_i.

Distance based method

The distance based method reduces the maximum length by a factor $(1-I)$ when $SDP = 1$, so $0 \leq ||x_j|| \leq \frac{(1-I)}{2}$. This is also changes the integral bounds. This gives us

$$\mathbb{E}_{x_j}[p(w_i,w_j,x_i,x_j)] = 2\int_0^{\frac{1}{2}(1-I)} (\frac{w_i w_j}{W||x_i-x_j||} \wedge 1)^{\alpha}\, dx_j$$
$$= 2\int_0^{\frac{1}{2}(1-I)} (\frac{w_i w_j}{W||x_j||} \wedge 1)^{\alpha}\, dx_j.$$

Again, $r_0 = \frac{w_i w_j}{W}$, but $0 \leq ||x_j|| \leq \frac{(1-I)}{2}$. So if $r_0 \geq \frac{(1-I)}{2}$, the integrand is 1. This gives us

$$\mathbb{E}_{x_j}[p(w_i,w_j,x_i,x_j)] = 2\int_0^{\frac{(1-I)}{2}} dx_j = (1-I).$$

If $r_0 < \frac{(1-I)}{2}$:

$$\mathbb{E}_{x_i,x_j}[p(w_i,w_j,x_i,x_j)]$$
$$= 2\int_0^{r_0} (\frac{r_0}{||x_j||} \wedge 1)^{\alpha} dx_j + 2\int_{r_0}^{\frac{1}{2}(1-I)} (\frac{r_0}{||x_j||} \wedge 1)^{\alpha} dx_j$$
$$= 2\int_0^{r_0} 1\, dx_j + 2\int_{r_0}^{\frac{1}{2}(1-I)} (\frac{r_0}{x_j})^{\alpha} dx_j$$
$$= 2(r_0 + r_0^{\alpha}\int_{r_0}^{\frac{1}{2}(1-I)} \frac{1}{x^{\alpha}} dx)$$
$$= 2(r_0 + r_0^{\alpha}[\frac{x^{1-\alpha}}{1-\alpha}]_{r_0}^{\frac{1}{2}(1-I)})$$
$$= 2r_0 + \frac{2^{\alpha} r_0^{\alpha}(1-I)^{1-\alpha} - 2r_0}{1-\alpha}$$
$$= r_0(2+\frac{2}{\alpha-1}) + O(r_0^{\alpha}).$$

So we conclude

$$\mathbb{E}_{x_i,x_j}[p(w_i,w_j,x_i,x_j)] = \begin{cases} 1-I, \text{ if } w_j \geq \frac{(1-I)W}{2w_i} \\ \frac{2w_i w_j}{W}(1+\frac{1}{\alpha-1}) + o(\frac{w_i w_j}{W}), \text{otherwise} \end{cases}.$$

Integrating over the weight gives us

$$
\begin{aligned}
&\mathbb{E}_{w_j}[\mathbb{E}_{x_i,x_j}[p(w_i,w_j,x_i,x_j)]] \\
&\approx \int_1^{\frac{(1-I)W}{2w_i}} (1+\frac{1}{\alpha-1})\frac{2w_i}{W} w^{-\gamma+1} dw + \int_{\frac{(1-I)W}{2w_i}}^{\infty} (1-I) w^{-\gamma} dw \\
&= (1+\frac{1}{\alpha-1})\frac{2w_i}{W}(\frac{(\frac{(1-I)W}{2w_i})^{2-\gamma}-1}{2-\gamma}) + (1-I)\frac{(\frac{(1-I)W}{2w_i})^{1-\gamma}}{\gamma-1} \\
&= (1+\frac{1}{\alpha-1})\frac{2w_i}{W(\gamma-2)} + 2(1+\frac{1}{\alpha-1})(1-I)^{2-\gamma}(\frac{(\frac{W}{2w_i})^{1-\gamma}}{\gamma-2}) \\
&+(1-I)^{2-\gamma}\frac{(\frac{W}{2w_i})^{1-\gamma}}{\gamma-1} \\
&= (1+\frac{1}{\alpha-1})\frac{2w_i}{W(\gamma-2)} + O((\frac{w_i}{n})^{\gamma-1}).
\end{aligned}
$$

So, in the limit the influence of the distance based intervention method disappears.

Weight based method
In the weight based method we multiply the weights with a factor $(1-I)$, when $SDP = 1$. This leads to

$$
\begin{aligned}
&\mathbb{E}_{x_j}[p(w_i,w_j,x_i,x_j)] = 2\int_0^{\frac{1}{2}} (\frac{(1-I)^2 w_i w_j}{(1-I)W||x_i-x_j||} \wedge 1)^{\alpha}\ dx_j \\
&= (1-I)\cdot 2\int_0^{\frac{1}{2}} (\frac{w_i w_j}{W||x_j||} \wedge 1)^{\alpha}\ dx_j.
\end{aligned}
$$

This means that our original expectation is now multiplied with a factor $(1-I)$. This factor will not influence the rest of the calculations, so we can conclude that all expected degrees are decreased by a factor $(1-I)$. This means that the weight based method proportionally decreases social connections. High-degree nodes will lose more edges than low-degree nodes in total, but proportionally they lose they same percentage of edges.

5.2 SIS equilibrium

The SIS model tends to end up in an equilibrium state, where the amount of infected and susceptible individuals is stable. In a SIS model without underlying network structure, we can exactly find this equilibrium. If our infection probability is β and our recovery probability is δ, we can set up the following differential equations to find the equilibrium, as we have seen in Section 2.1.2:

$$\frac{dS}{dt} = \delta \cdot I - \beta \cdot S \cdot I \cdot N = -\frac{dI}{dt} \tag{24}$$

To find the equilibrium of this model, we need to set $\frac{dI}{dt} = 0$. This results in

$$S \cdot I \cdot \beta \cdot N = \delta \cdot I. \tag{25}$$

Since $S = 1 - I$, we can substitute this, and we find $I = 1 - \frac{\delta}{\beta \cdot N}$.

As mentioned before, in the compartment model without network structure, every individual can infect any other individual in the system. This is a highly unlikely, since people only meet a limited amount of individuals of the total population. To account for this in the equilibrium calculations, we need to introduce a term Θ, which is the probability that a healthy node links to an infected node. To exactly find the equilibrium of a SIS epidemic on a given graph, we would need to set up differential equations for every node, which would describe the relations with its neighbours. Since this is not feasible, we make the assumption that nodes with the same degree behave similarly. With this assumption we can set up differential equations for the density of infected nodes ρ_k for a given degree k:

$$\frac{d\rho_k}{dt} = -\rho_k + \lambda k(1 - \rho_k)\Theta, \tag{26}$$

where $\lambda = \frac{\beta}{\delta}$, and Θ is the probability that any given edge points to an infected node. The $-\rho_k$ term covers the recovered nodes. The $\lambda k(1 - \rho_k)\Theta$ term is the expected number of healthy nodes with degree k that get infected by an infected neighbour. To find the equilibrium, we check when $\frac{d\rho_k}{dt} = 0$. This results in

$$\rho_k = \frac{k\lambda\Theta}{1 + k\lambda\Theta}. \tag{27}$$

Since Θ is the probability that a healthy node links to an infected node, we get

$$\Theta = \frac{\sum_k kP(k)\rho_k}{\mathbb{E}(k)}, \tag{28}$$

where $P(k)$ is the probability of a node with degree k, and $\mathbb{E}(k)$ is the expected degree. Since our networks follow a power law, $P(k) = k^{-\gamma}$, with $2 < \gamma \leq 3$. For calculation purposes, we will set $\gamma = 3$. Filling in equation 27 in equation 28 gives

$$\Theta = \sum_k \frac{\lambda\Theta}{\mathbb{E}(k)(k + k^2\lambda\Theta)} \tag{29}$$

$$\Theta\,\mathbb{E}(k)\lambda^{-1} \approx \int_1^\infty \frac{\Theta}{k + k^2\lambda\Theta} dk \tag{30}$$

$$= \Theta \log(\frac{\lambda\Theta + 1}{\lambda\Theta}) \tag{31}$$

$$\Theta = \frac{1}{\lambda(e^{\mathbb{E}(k)\lambda^{-1}} - 1)} \tag{32}$$

If we fill in this Θ in the formula for ρ_k, we get

$$\rho_k = \frac{k}{e^{\mathbb{E}(k)\lambda^{-1}} + k - 1}. \tag{33}$$

This formula is for a given degree k, so to find our general equilibrium, we need to average over k:

$$\rho = \sum_k \rho_k P(k) \tag{34}$$

$$= \sum_k \frac{k^{-2}}{e^{\mathbb{E}(k)\lambda^{-1}} + k - 1} \tag{35}$$

$$\approx \int_1^\infty \frac{k^{-2}}{e^{\mathbb{E}(k)\lambda^{-1}} + k - 1} dk \tag{36}$$

$$= \frac{e^{\mathbb{E}(k)\lambda^{-1}} - \mathbb{E}(k)\lambda^{-1} - 1}{(e^{\mathbb{E}(k)\lambda^{-1}} - 1)^2} \tag{37}$$

Expression 37 gives us an approximated analytical solution for the equilibrium of the SIS model, but only for the situation where the virus can spread freely, and no interventions are implemented. To be able to analytically calculate the SIS equilibrium with interventions, we must carefully choose the intervention strategy. All the interventions that delete edges, and thus change our network, cannot easily be implemented in the differential equations. The calculations above assume that the node degrees are fixed, while by deleting edges the node degrees will change. The only intervention strategy that does not change the network structure is varying the infection probability based on the prevalence, which is explained in more detail in section 4.2.3. If $SDP = 1$, β will be a function of the prevalence ρ: $\beta = \beta_0(1-\rho_k)$, where β_0 is the infection probability without interventions. Since $\lambda = \frac{\beta}{\delta}$, $\lambda = \lambda_0 \cdot (1 - \rho_k)$. Substituting this is equation 26 when $\frac{d\rho_k}{dt} = 0$ gives $\rho_k = \lambda(1 - \rho_k)^2 k\Theta$. Solving for ρ_k gives

$$\rho_k = \frac{-2\Theta k\lambda + \sqrt{4\Theta k\lambda + 1} - 1}{2\Theta k\lambda}. \tag{38}$$

Filling in the equation for ρ_k in equation 28 for Θ gives

$$\Theta\,\mathbb{E}(D) = \sum_k \frac{-2\Theta k\lambda + \sqrt{4\Theta k\lambda + 1} - 1}{2\Theta k^4\lambda} \tag{39}$$

$$\approx \int_1^\infty \frac{-2\Theta k\lambda + \sqrt{4\Theta k\lambda}}{2\Theta k^4\lambda} \tag{40}$$

$$= -\frac{1}{2} + \frac{2}{5\sqrt{\Theta\lambda}}. \tag{41}$$

Solving for Θ gives a long expression that will not be written down, but it can be used to numerically calculate the expected equilibrium value, by substituting it in equation 38, and average over k.

6 Simulation results

This section investigates the effectiveness of the adaptive intervention strategies by comparing key metrics across multiple parameter settings and scenarios. The focus lies on understanding the trade off between controlling the epidemic and the societal impact.

6.1 Key metrics

To assess the effectiveness of our intervention strategies, we need to indicate a list of key metrics. We will focus on the following metrics:

Time and height of the peak: The number of people infected at the peak of the epidemic is crucial for hospitals. If the peak is too high, hospitals might not have enough capacity to treat everyone. During the COVID-19 pandemic, one of the main focus points was to lower and delay the peak of the infection, under the name *flatten the curve*. If the peak of the epidemic is very early, not much will be known about the disease, and hospitals might be less prepared. The later the peak of the disease is, the more time hospitals have to prepare for the peak. We denote the peak height by $I_{max} = \max_{t \geq 1} I_t$, and the time of the peak $t_{max} = \arg\max_{t \geq 1} I_t$.

Total infections: The number of people that have been infected during the epidemic is of main importance, since it gives a clear view of the size of the outbreak. For the SIR model, the total number of infections is exactly the number of recovered individuals at the final time step. For the models where reinfection is possible, such as SIS and SITS, the total infections are counted. This means that the total infections can be higher than the total population size. We refer the total number of infections by I_{total}.

Epidemic duration and second peaks: If the duration of an epidemic is short, the disruption by it is generally small. The longer it is takes to eradicate a disease, the more influence it will have on society. In the SIS and SITS models, multiple peaks often occur, due to the ability of moving back to the Susceptible compartment. It can be the case that an intervention strategy does have a positive influence on some of the metrics, but does cause multiple waves to occur. This can lead to a prolonged epidemic duration, which can be undesirable.

We need to specify what we consider to be peaks, since we do not want to count every minor fluctuation in the data as a peak. We exclude small fluctuations by setting a threshold value on the prominence, also known as the relative height. The prominence of a peak is defined as the minimum drop in height necessary in order to reach a higher point in the data. Mathematically, for a peak at time t with height $h(t)$, the prominence is defined as

$$P(t) = h(t) - \min(h_{\text{min, left}}, h_{\text{min, right}}), \tag{42}$$

where $h_{\text{min, left}}$ and $h_{\text{min, right}}$ are the lowest points encountered when descending from t to any higher peak on the left and right, respectively. We set a threshold value P_{thresh} to say a peak at time t is significant if

$$P(t) > P_{\text{thresh}}. \tag{43}$$

.

This leads to small fluctuations being ignored as peaks.

Societal impact: The way to measure societal impact depends on the intervention method. The weight based, distance based and random percolation intervention methods depend on deleting edges from the network. Deleting edges can be seen as decreasing social contacts, which has a societal impact. The metric to measure societal impact due to edge deletion will be the edge ratio

$$R_{E,t} = \frac{|E_t|}{|E|}, \tag{44}$$

where $|E|$ is the size of the graph at the begin of the epidemic, and $|E_t|$ the size of the graph at time t. If $R_{E,t}$ is low, it means that a lot of edges are deleted, so the societal impact is high. The societal impact per time step can be expressed as

$$SI_{E,t} = 1 - \frac{|E_t|}{|E|}. \tag{45}$$

If we sum this over the duration of the pandemic, we get the total societal impact

$$SI_E = \sum_{t=1}^{T}(1 - \frac{|E_t|}{|E|}). \tag{46}$$

This gives a clear indication of the strength of the interventions, as well as the length of the epidemic.

The infection probability intervention method does not delete edges, but lowers the infection probability. We can measure its impact in a similar fashion as the edge reduction methods.

$$R_{\beta,t} = \frac{\beta_t}{\beta} \tag{47}$$

measures the ratio of the infection probability per time step.

$$SI_{\beta,t} = 1 - \frac{\beta_t}{\beta} \tag{48}$$

is then the societal impact per time step, and finally

$$SI_\beta = \sum_{t=1}^{T}(1 - \frac{\beta_t}{\beta}) \tag{49}$$

sums over the societal impact per time step to get the total societal impact. We can now directly compare edge reduction methods and the infection probability method, since both SI_E and SI_β are the sum of the relative societal impact. For the local infection probability method, we take the average of the infectiousness per individual

$$\beta_t = \frac{\sum_{v \in V} \beta_{v,t}}{n}. \tag{50}$$

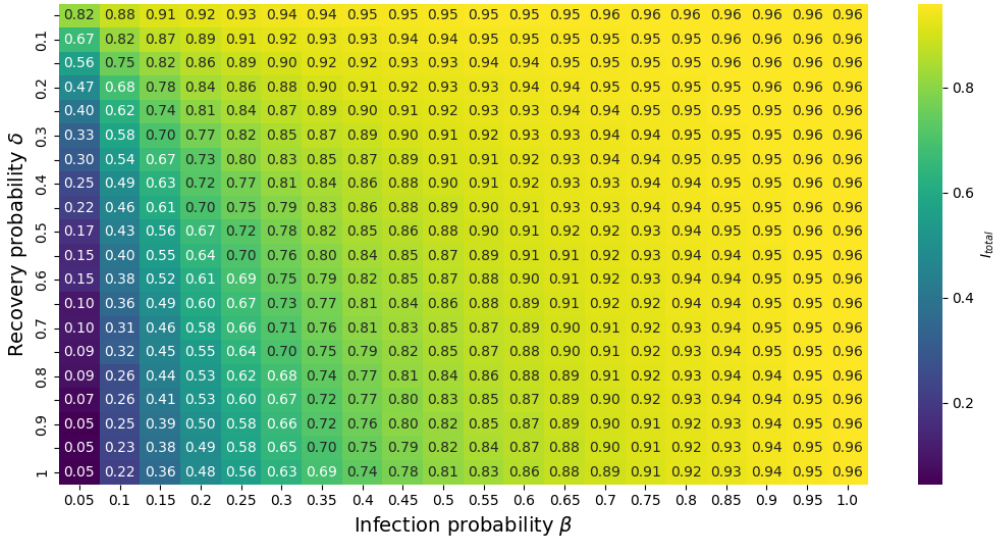

FIGURE 2: Heat map of I_{total} for different values of β and δ, using the SIR model without interventions

6.2 Parameter choices

Since the number of possible parameter combinations is vast, we select parameter values that align with realistic epidemic scenarios. In this section we are mainly interested in the course of diseases like COVID-19, but with the choice of different parameters, other disease classes could also be simulated. However, this is beyond the scope of this thesis.

Infection and recovery probability

Two crucial characteristics of a disease are the infection probability β and the recovery probability δ. In Figure 2 we see a heat map of the ratio of the total number of infections I_{total}, for a SIR epidemic on a GIRG with 1000 nodes, without interventions. We see that for $\beta > 0.75$ the recovery rate does not have a lot of influence, since the ratio of the total number of infections lies above 0.9. For a low infection probability, the recovery rate has a large influence. Since in general, the recovery period of COVID-19 lies around 5 to 10 days [4], we will set the recovery rate to $\delta = 0.15$. Closely related studies, such as Jorritsma et al. [14] use an infection probability that is close to the recovery probability, so we will use $\beta = 0.15$.

Network

For the simulations, we will use networks with 1000 vertices. This size results in complex networks that are still small enough to simulate disease spread within a reasonable time frame. Next to the network size, we need to choose the average degree $\mathbb{E}[\deg(v)]$, and the value for α. We will set $\mathbb{E}[\deg(v)] = 8$, in accordance with Jorritsma et al. [14]. We will set $\alpha = 1000$, which would have the same effect as any other arbitrary large value for α (see equation 14).

Social distance power

The social distance power (SDP) determines the effectiveness of the intervention strategies. We will use different values of SDP for the simulations, to give a clear view of the effect of this parameter.

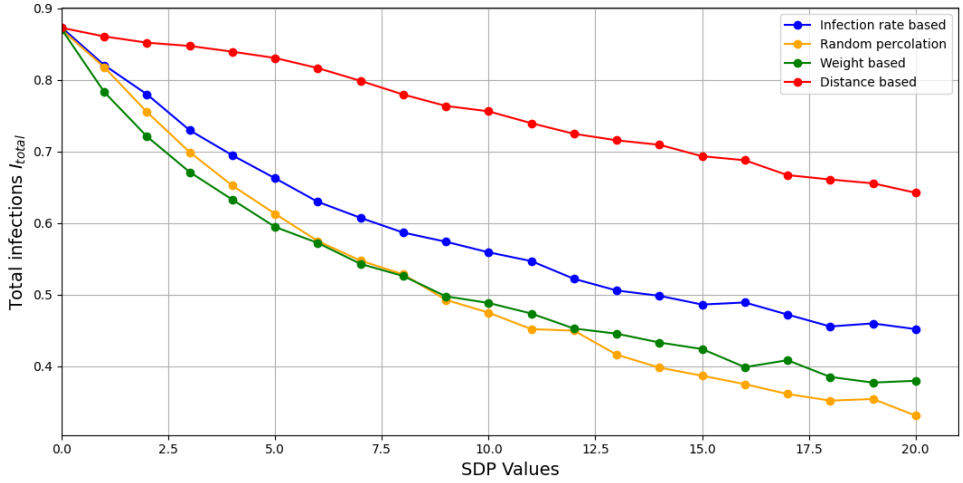

FIGURE 3: Total infections with different values of SDP, for SIR simulation of the 4 methods. Averages are taken over 50 simulations per data point.

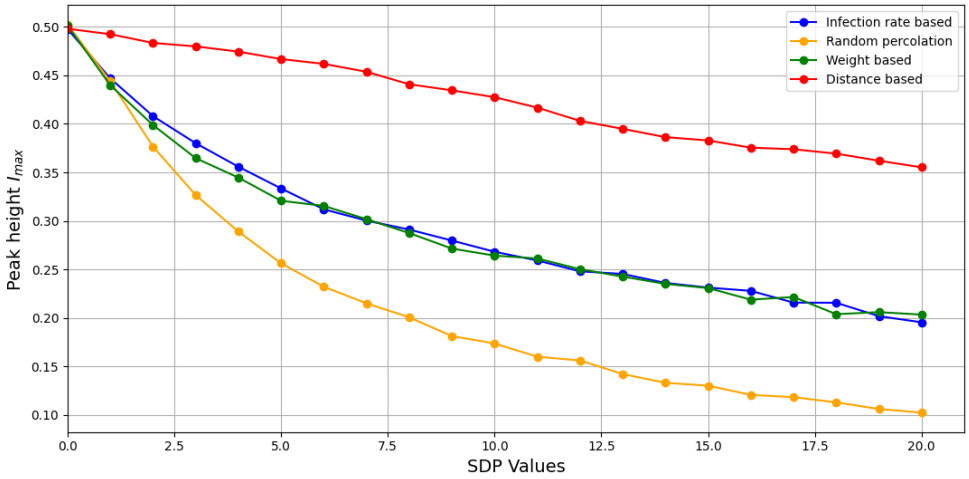

FIGURE 4: Peak infections with different values of SDP, for SIR simulation of the 4 methods. Averages are taken over 50 simulations per data point.

Other parameters

To prevent the disease from dying out before infecting anyone, we set the number of infections at the start to 10. Model specific parameters, such as the immunity loss probability η, will be specified when used.

6.3 Comparison of intervention strategies

Now that the majority of the parameters is fixed, we can use them to compare our intervention strategies. In Figure 3 we see the average number of total infections of the four methods in a SIR simulation. For every point, the average is taken over 50 simulations. For these simulations, the parameters are as described previously. In Figure 4 we see the average height of the peaks of the same simulations.

We see that for all four methods the total infections decrease as SDP gets bigger,

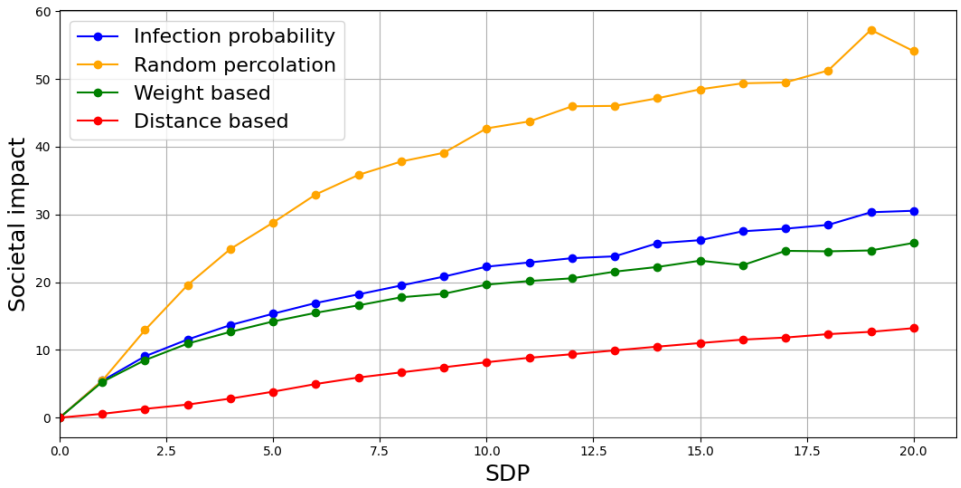

FIGURE 5: Total societal impact for different values of SDP, for SIR simulation of the 4 methods. Averages are taken over 50 simulations per data point.

which is as expected. We see that the random percolation and weight based methods generate the lowest I_{total}, while the distance based method has significantly larger outcomes. The random percolation method has significantly lower peaks, while the peak heights for the weight and infection probability methods are remarkably similar. One could think this means that the distance based method is the least efficient of the four methods, but this is not necessarily true. What this figure does not show is the societal impact. Since the algorithms have a different implementation of the SDP parameter, the effect on the methods might not be equivalent. In Figure 5 we see the societal impact of the simulations.

We see that the distance based method has a significantly lower societal impact, while the random percolation method has a substantial societal impact. The weight based method and infection probability method show very similar societal impact. To fairly compare the four methods, we want to select SDP values for which all the methods have a similar societal impact. If we take a societal impact of 10, we approximately get $SDP = 1.65$ for random percolation, $SDP = 2.5$ for weight based, $SDP = 2.4$ for infection probability based, and $SDP = 13$ for distance based. Per method, we run 200 simulations, and plot the average disease trajectories. In Figure 6 we see the averaged disease trajectories of the four methods laid over each other. Here we see that the weight based method leads to the lowest total number of infections, while the distance based method is the most effective method when it comes to reducing the peak. The random percolation method is the least effective in both decreasing the peak and decreasing the total number of infections.

In the left picture of Figure 7 we see the average societal impact per time step. We clearly see that the distance based method creates a much stronger initial intervention, but it is also released earlier than the other methods. This causes the total societal impact for the different methods to be similar. This can be seen in right picture of Figure 7, where the cumulative societal impact per method is plotted. We see that at the end of the epidemic, the total societal impacts per method are very similar, which is desirable if we want to fairly compare the effectiveness of the methods.

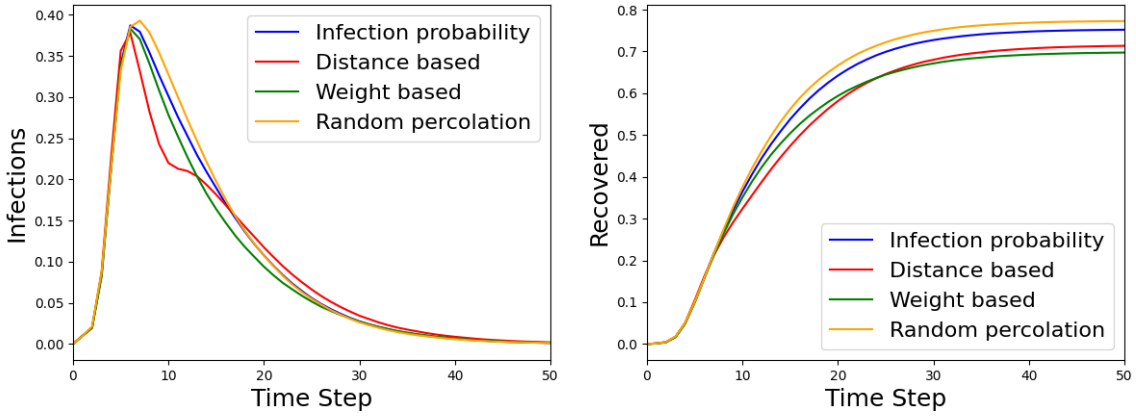

FIGURE 6: SIR Disease graphs of the four methods with $SDP = [2.4, 13, 2.5, 1.65]$ respectively. Left: Infections. Right: Recovered. Averages are taken over 200 simulations per method.

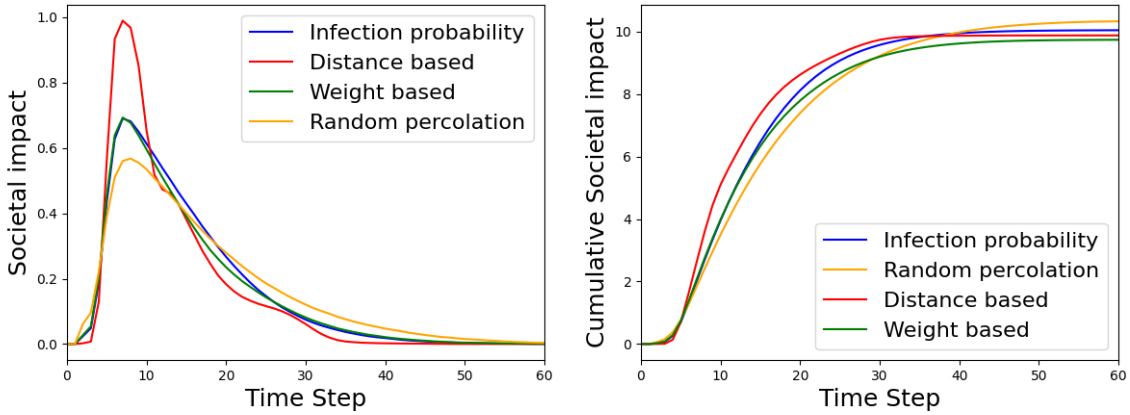

FIGURE 7: SIR Societal impact graphs of the four methods with $SDP = [2.4, 13, 2.5, 1.65]$ respectively. Left: Societal impact per time step. Right: Cumulative societal impact. Averages are taken over 200 simulations per method.

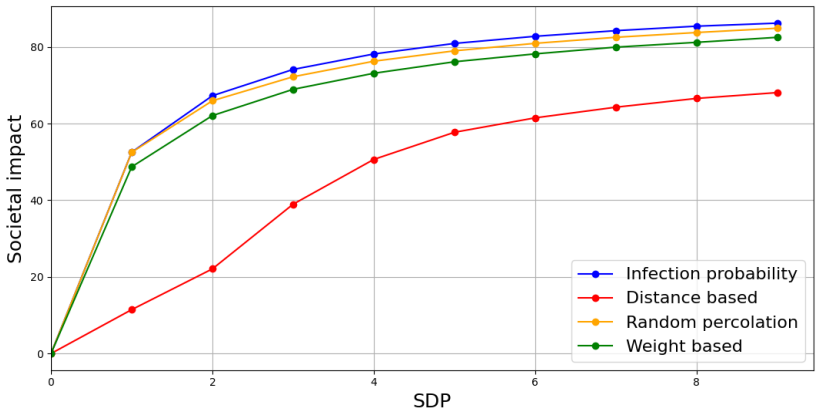

FIGURE 8: Total societal impact plotted against different SDP values for the four methods, on the SIS model. Averages are taken over 50 simulations per data point.

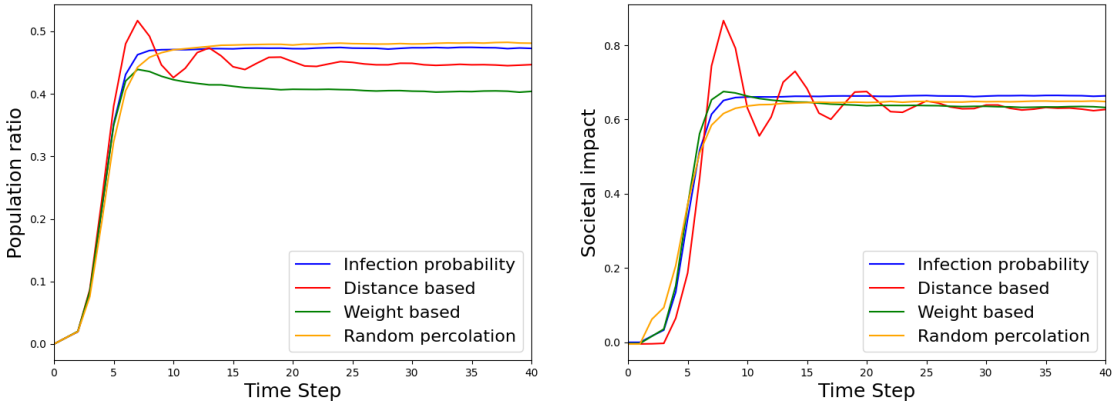

FIGURE 9: SIS Societal impact graphs of the four methods with $SDP = [1.7, 6, 2, 1.7]$ respectively. Left: Societal impact per time step. Right: Cumulative societal impact. Averages are taken over 200 simulations per method.

SIS

In the SIS model, recovered individuals become susceptible immediately. To see the effect of the different social distancing models, we again plot the societal impact per SDP value, which can be seen in Figure 8. We can now choose SDP values to let the four methods have a similar societal impact. We set $SDP = 6$ for distance based, $SDP = 2$ for weight based, and $SDP = 1.7$ for the infection probability and random percolation methods.

In Figure 9 we see the infections curves for these values of SDP and the corresponding societal impact. We notice that with the distance based intervention, the disease has multiple peaks before it reaches an equilibrium. The other methods reach their equilibrium already after the first peak. This can be explained by the fact that the distance based method 'overshoots' the equilibrium with stronger interventions, and then also releases the interventions too quickly. We also notice that with similar societal impact, the weight based method leads to the lowest equilibrium of infections.

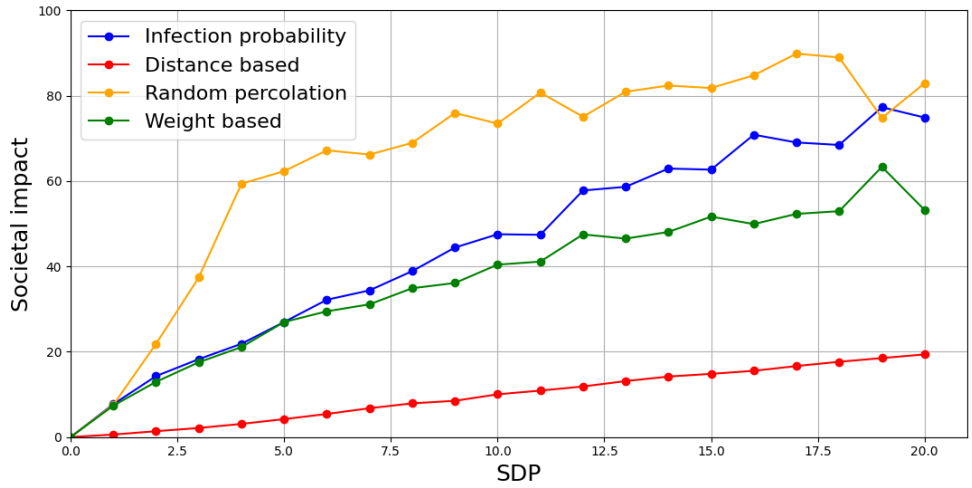

FIGURE 10: Total societal impact for different values of SDP, for SITS simulation of the 4 methods. Averages are taken over 50 simulations per data point.

SITS

For the SITS model we need to fix the average length of immunity, which determines the parameter η, which is the probability of losing immunity. We choose the average length of immunity to be 120 days, which is reasonable according to the Association of American Medical Colleges [3]. This gives $\eta = \frac{1}{120}$. We again simulate the disease spread for multiple values of SDP. The peak infections are practically the same as in Figure 4, since the deimmunization has almost no effect on the initial peak. In Figure 10 we see the societal impact for increasing values of SDP per method. We see again see that the random percolation method causes the most societal impact, and the distance based method the least. We take SDP values 2, 4, 4.1, and 22 for random percolation, infection probability based, weight based and distance based, respectively, since this leads to similar societal impact.

In Figure 12 we see the societal impact per time step and the cumulative societal impact. Similar to the SIR simulations, the distance based method has a higher societal impact peak, but cumulative it is comparable to the other methods. In Figure 11 we see the averaged SITS curves relating to the four methods. Since the curves are averaged over 200 simulations per method, possible second peaks in single simulations are not visible. In Figure 13 we see some data about second peaks in the simulations. We see that with the distance based method the average number of peaks is higher, as well as the average height and time of the second peaks.

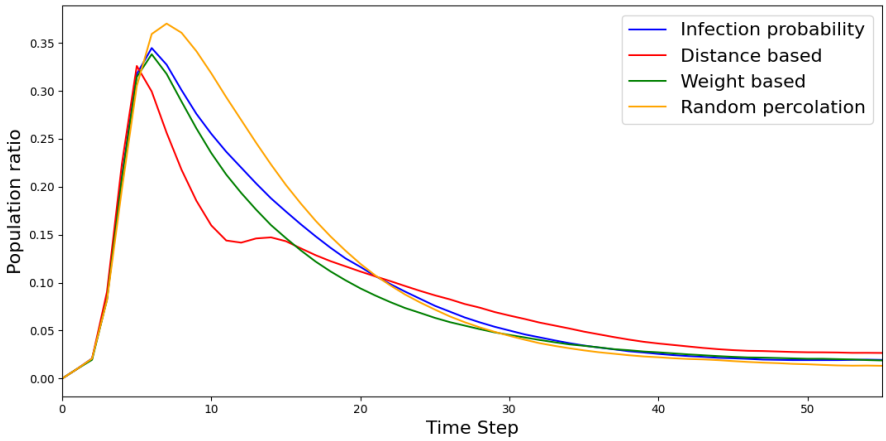

FIGURE 11: SITS Infection graphs of the four methods with $SDP = [4, 22, 4.1, 2]$ respectively. Averages are taken over 200 simulations per method.

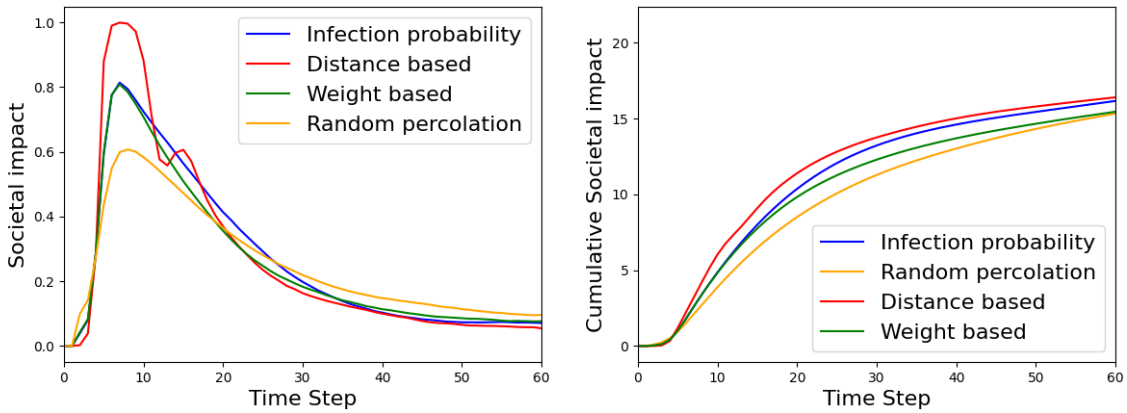

FIGURE 12: SITS societal impact graphs of the four methods with $SDP = [4, 22, 4.1, 2]$ respectively. Left: Societal impact per time step. Right: Cumulative societal impact. Averages are taken over 200 simulations per method.

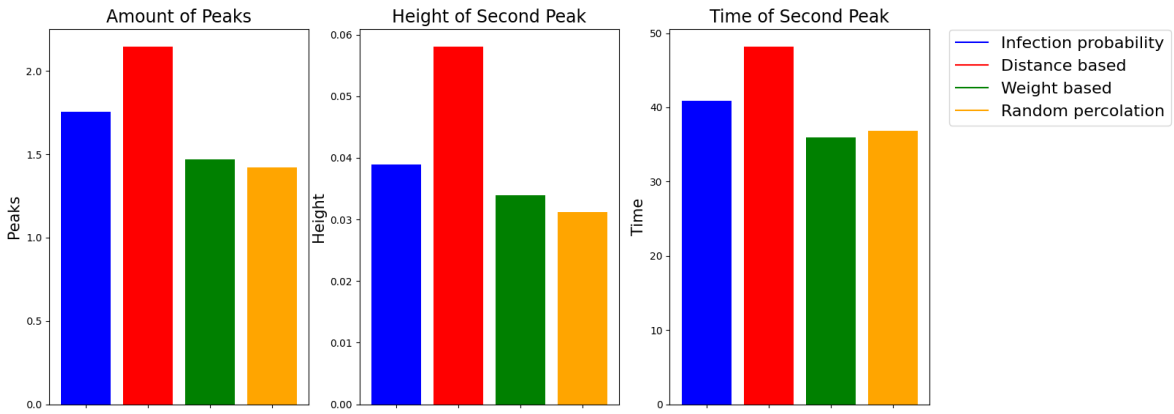

FIGURE 13: Bar plots for the number of peaks, height of the second peaks and the time of the second peak, for the SITS simulations. Averages are taken over 200 simulations per method.

6.4 Effect of local information

The local information option has been implemented for the distance based method and infection probability method. In Figure 14 we see the disease trajectories of the local methods plotted against the global methods. This is again done with the same parameters as in Section 6.3, on the SIR model. We see that the local methods result in lower peaks. Especially the local distance based method mitigates the disease spread substantially. On the left picture of Figure 15 we see the comparison of the societal impact. We see that the local methods start earlier, but have less strict intervention peaks than their global counterparts. However, the local distance intervention method goes on for a longer period. On the right picture of Figure 15 we see the cumulative societal impact. Since the local distance based method continues for a longer time, the total societal impact is higher. Interestingly, the local infection probability method outperforms its global counterpart in all metrics. It delays the peak, the peak is lower, and the number of total infections is lower. Additionally, it has a lower societal impact than the global version.

To more fairly assess the difference between the global and local distance based methods, we want to choose a lower SDP value for the local distance based method. In Figure 16 we see the SIR curves for the distance based method, now including the local distance based method with $SDP = 6$ and $SDP = 8$. We see that for these values, the local method still outperforms its global counterpart. In Figure 17 we see the corresponding societal impact plots. While for $SDP = 13$ the local method had a higher societal impact, for $SDP = 6$ and $SDP = 8$ the societal impact is lower than for the global method. So, we conclude that for these parameter settings, the local method is outperforming the global method in both peak reduction, total infections and societal impact, for the distance based method, as well as for the infection probability based method.

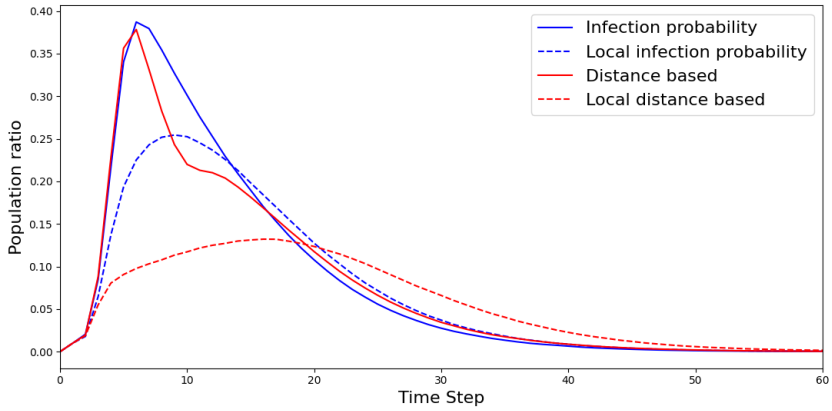

FIGURE 14: Infection plots of SIR simulations for the infection probability method and the distance based method, for local and global methods. $SDP = 13$ for the distance based method, $SDP = 2.4$ for the infection probability method. Averages are taken over 200 simulations per method.

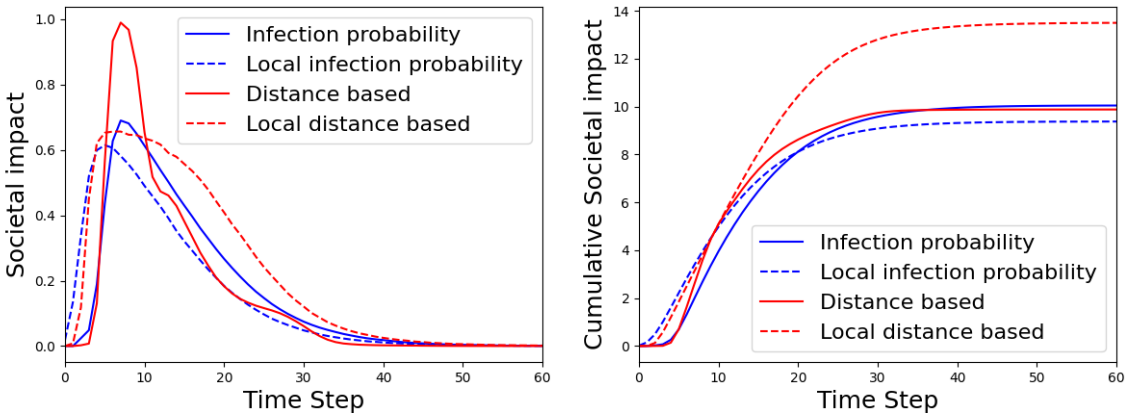

FIGURE 15: Societal impact plots of SIR simulations for the infection probability method and the distance based method, for local and global methods. $SDP = 13$ for the distance based method, $SDP = 2.4$ for the infection probability method. Left: societal impact per time step. Right: cumulative societal impact.

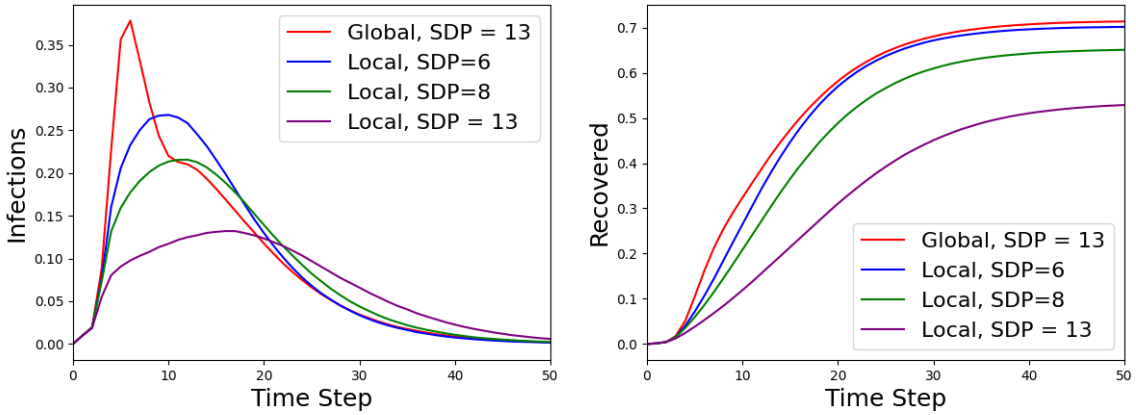

FIGURE 16: SIR disease graphs of the global and local distance based method. Left: infections part of the population. Right: recovered part of the population. Averages are taken over 200 simulations per method.

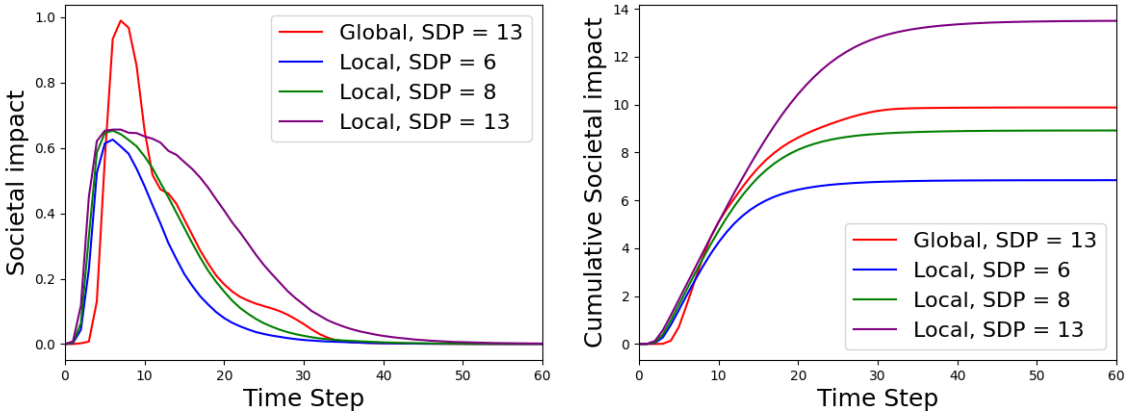

FIGURE 17: Societal impact graphs of the global and local distance based method. Right: societal impact per time step. Left: cumulative societal impact. Averages are taken over 200 simulations.

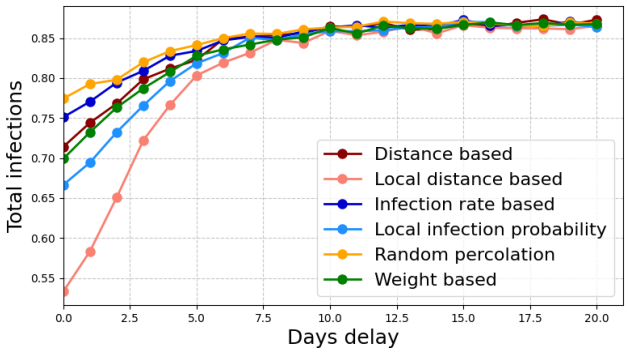

FIGURE 18: Total SIR infections plotted against days delay for multiple methods. The average is taken over 50 simulations per data point.

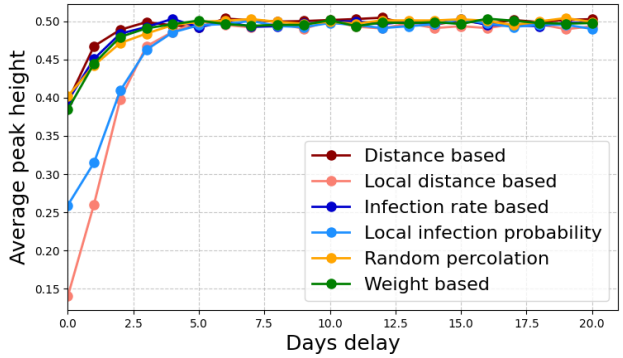

FIGURE 19: Peak SIR infections plotted against days delay for multiple methods. The average is taken over 50 simulations per data point.

6.5 Effect of delay

When modelling delay, we have to make the parameter choice of how much delay there is. To give a clear overview of the effect of delay on the four models and the two local versions, Figure 18 shows the total infections per value of delay, per intervention method. We see that for all the methods the total infections increase as the delay increases. Since the delay causes a slower reaction to the disease, this is as expected. Interestingly, after more than seven days of delay, all the methods converge to same number of total infections, which implies that the intervention methods are practically useless. This makes sense, since the peak of the disease spread in the simulations often lies before day 10. In Figure 19 we see the height of the peak for different delay values. We again see similar behaviour: the values converge quickly, now for 5 or more days delay.

Strictly enforcing interventions, and releasing them quickly after the peak could possibly lead to second peaks. To test if there are scenarios in which delay can have any positive effect, we set up the following experiment. To get a 'slower' disease, we choose an infection probability of $\beta = 0.03$ and recovery probability of $\delta = 0.05$. Next to that, we start the disease with 5 instead of 10 initial infections. We now simulate a SITS disease for different values of delay and SDP, for the different methods. In Figure 20 we see the heat map of the global infection method of these simulations, with the total infections as metric. Every

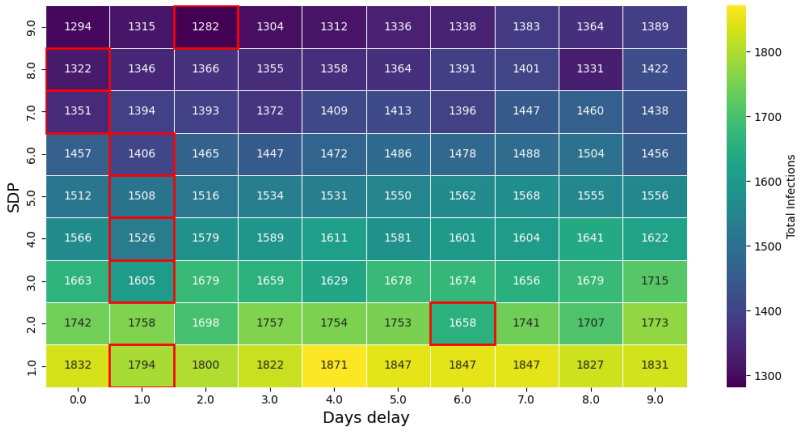

FIGURE 20: Heat map of SITS total infections for the global infection probability method, for different SDP and delay values, with $\beta = 0.03$ and $\delta = 0.05$. For every data point, the average is taken over 50 simulations. The lowest value per row is outlined in red.

data point is the average of 50 simulations. Outlined in red we find the lowest value in each row, so for each value of SDP.

We already see there are situations in which there are values of delay for which the total infections is lower than for zero delay. Since these simulations are stochastic, this can occur without the result being significant. In Figure 20 we see multiple rows, so values of SDP for which the lowest value is at a delay value bigger than zero. To see how significant this result is, we now do 100 simulations per parameter combination, and plot the total infections including a 95% confidence interval for the expected mean of these 100 simulations. In Figure 21 we see the graphs of this. We see that the mean value sometimes is smaller for a non-zero value of delay. But, the confidence intervals are wide enough that the lowest value can still be attained for zero days delay.

From this we conclude that for specific parameter settings, in some simulations, the outcomes might be a bit better when there is delay. But when the average is taken over multiple simulations, it cannot be shown to be a significant improvement. However, it is not always strictly outperformed by zero delay, as was the case in the simulations of Figure 18.

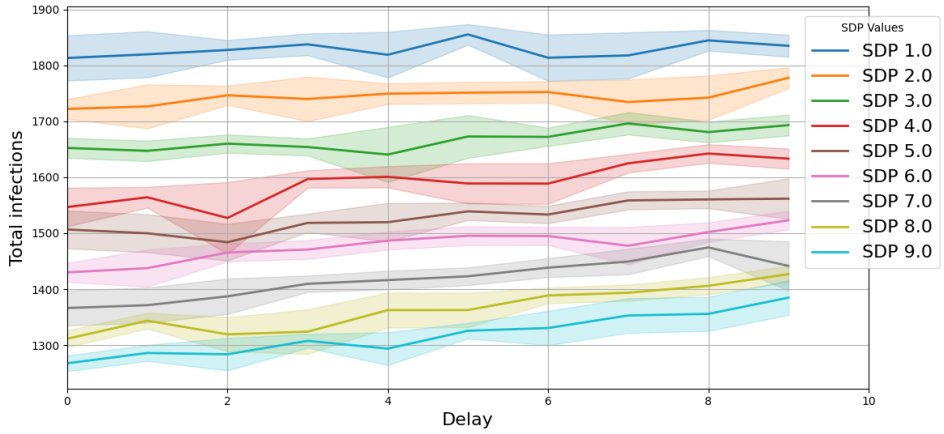

FIGURE 21: Total SITS infections per value of SDP and days delay, with a 95% confidence interval of the mean value, for the global infection probability method.

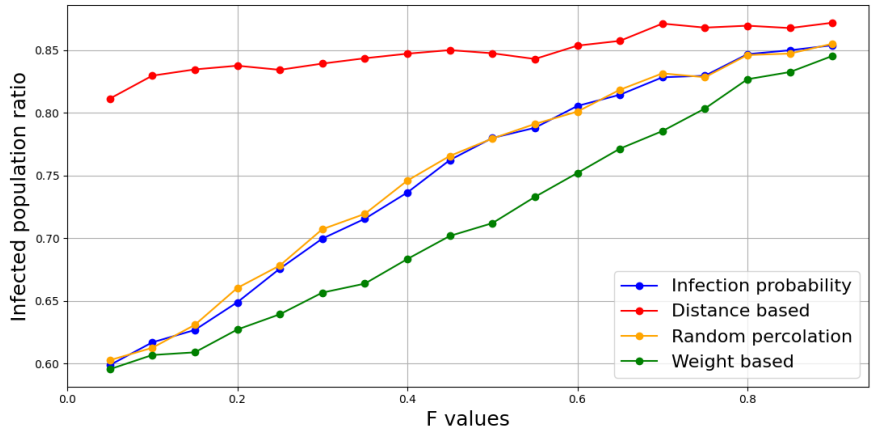

FIGURE 22: Total threshold infections plotted against different F values per method, with $M = 0.1$. Per data point, the average is taken over 50 simulations.

6.6 Adaptive compared to threshold

To compare our adaptive intervention methods with threshold methods, we need to set the parameters M and F. Recall from section 4.2.5 that M is the threshold on the infection prevalence after which the interventions will be instated, and that F decides the strength of the intervention. We arbitrarily choose to fix $M = 0.1$. We can then plot the influence of parameter F for the different methods. In Figure 22 we see the total infections of the disease for different F values. In Figure 23 we see the societal impact for different values for F.

If we want to compare threshold with adaptive methods, we need to pick values for SDP and F such that the total societal impact is similar. In Section 6.3 we set the values of SDP to get to a total societal impact of 10. To compare the threshold results with the adaptive results, we set the values for F to also end up with a societal impact of 10. We take $F = 0.4$ for the infection probability and random percolation methods, $F = 0.25$ for the weight based method, and $F = 0.027$ for the distance based method. Running simulations for these values gives the disease graphs as shown in Figure 24. In Figure 25

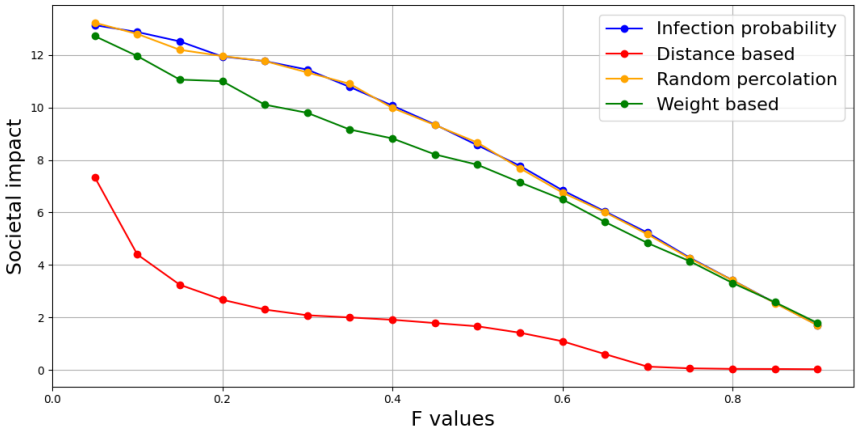

FIGURE 23: Threshold SIR societal impact plotted against different F values per method, with $M = 0.1$. Per data point, the average is taken over 50 simulations.

we see the corresponding societal impact. We can see that the cumulative societal impact is similar between the methods, so we can fairly compare them.

Interestingly, all the threshold methods lead to lower peaks than their adaptive counterparts. From Figure 24 we see that only the adaptive distance based model leads to slightly fewer infections than the threshold method, while for the other three methods the threshold model leads to fewer infections. Especially for the weight based method does the threshold method lead to a lower number of total infections.

Interestingly, the weight based model is performing the best of the four threshold methods, with stronger interventions, which are also released earlier. This leads to the same cumulative societal impact. Another interesting observation is the similarity of the infection probability method and the random percolation method. Even though the one method deletes edges, and the other lowers the infection probability, the infection curves as well as the societal impact curves are almost identical.

SIS threshold

In Figure 26 we see the societal impact of the four methods for different F values on the SIS model. Remarkable is the similarity between the infection probability method, the random percolation method and the weight based method. Only the distance based method has a different societal impact with the same F values. To fairly compare the methods, we set $F = 0.05$ for the distance based method, and find the corresponding value $F = 0.56$ for the other three methods. In Figure 27 we see the infection graph and the corresponding societal impact for the chosen F values. The societal impact of all the four methods is now almost equal. The infection graph of the weight based method is the only one that has a significantly lower equilibrium. The other three methods are again indistinguishable. In the long run, the adaptive and threshold methods are the same if the SIS equilibrium is larger than the threshold value. Because the infections are stable, the adaptive interventions are also stable, which is the same as in the threshold model. The only difference is that in the threshold model the intervention strength is predefined, while for the adaptive method, the infection equilibrium defines the intervention strength.

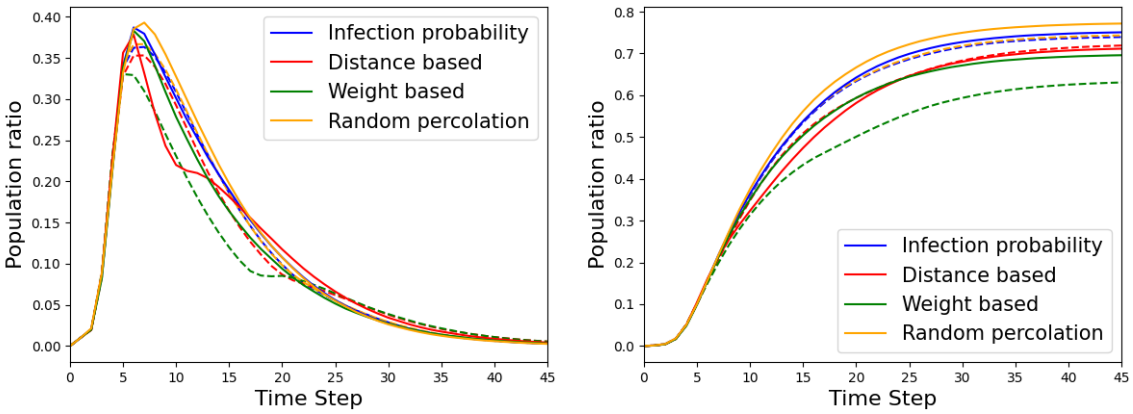

FIGURE 24: SIR Comparison of the adaptive (full lines) and threshold (dashed lines) methods. I (left) and R (right) curves for $M = 0.1$ and specific F values. Per line, the average is taken over 200 simulations.

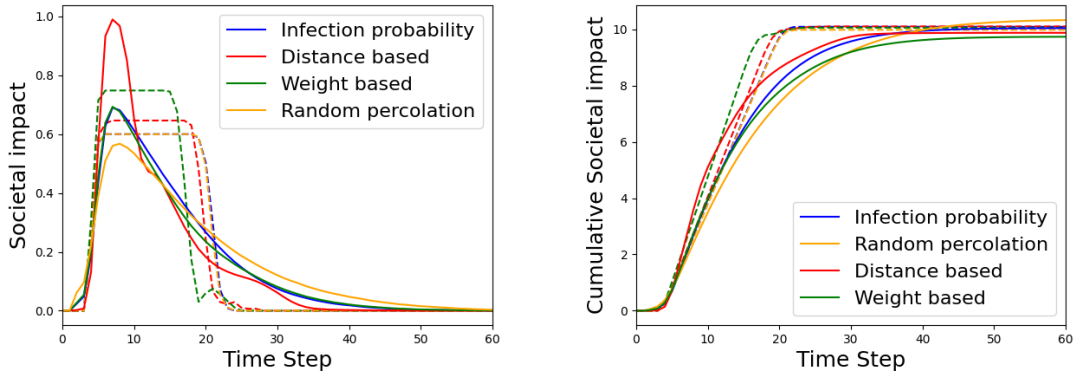

FIGURE 25: SIR Comparison of the societal impact of the adaptive methods and the threshold methods. The dashed lines are from the threshold methods, the full lines from the adaptive methods. For all lines, the average is taken over 200 simulations.

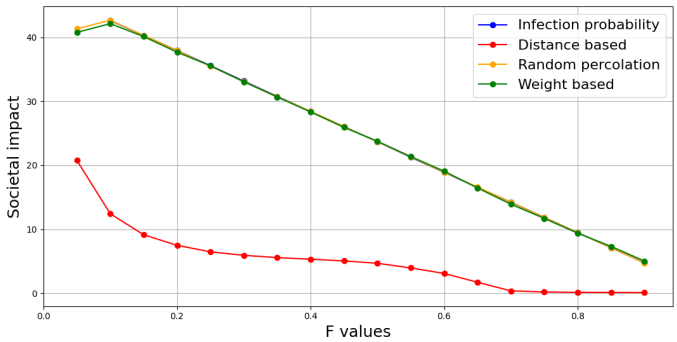

FIGURE 26: Threshold SIS Societal impact plotted against different F values. Per data point, the average is taken over 50 simulations.

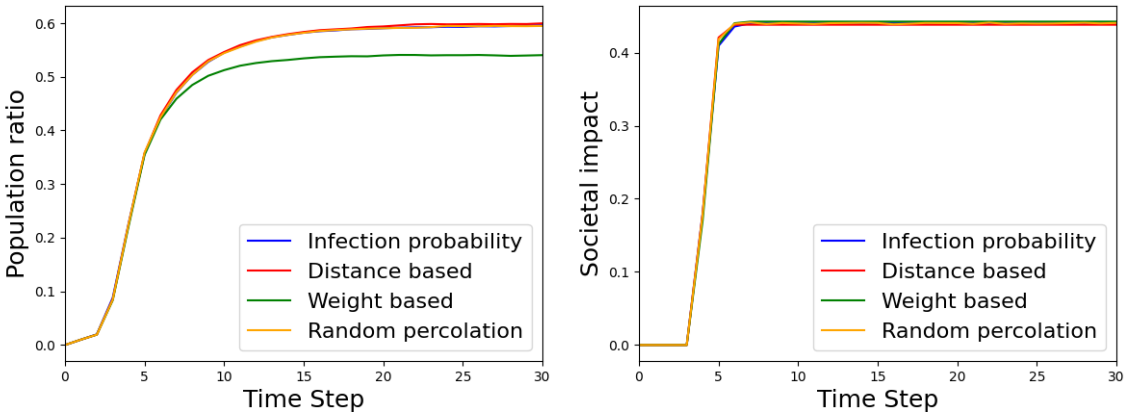

FIGURE 27: Threshold SIS infections (left) and societal impact (right), with $F = 0.05$ for the distance based method and $F = 0.56$ for the other methods. $M = 0.1$. For every line, the average is taken over 200 simulations.

6.7 Using flight data as input network

During pandemics, international flights are often reduced to prevent the spreading of the disease over multiple continents. Since the network of airports and airlines can be represented as a graph with geographical coordinates, we can use our model for geometric graphs on this dataset. The cities are the nodes of our network, and the flight segments between cities are the edges. We use data from SEES:lab [1]. Even though this data is from the year 2000, it still gives a good representation of today's international flight network. Since practically every flight route is taken in both directions, so from A to B and from B to A, the graph is regarded as undirected. This is helpful, since our network-based model is also created for undirected graphs.

The network consists of 3499 nodes and 27102 edges. This gives an average degree of 7.75. The node with the highest degree has a degree of 248. This node corresponds to Paris, France. Other cities in the top 5 of nodes with the highest degree include Frankfurt am Main, London, Amsterdam and Chicago. This seems plausible since these are all cities with large international airports.

We simulate a SIR disease over this network of airports. The distance based method is adjusted by changing the maximum distance $\sqrt{2}$ into 20000 km. The earth's circumference is roughly 40000 km, so by taking half of that, we get the maximum distance any flight route would be.To compare the influence of the network structure of the airports opposed to GIRGs, we use the same parameters as used in Figures 6 and 7.

In Figure 29 we see the outcomes of these simulations, and the corresponding societal impact graphs can be seen in Figure 30. If we compare them to Figures 6 and 7, we see that the outcomes are similar. This is as expected, since the average degree of the airport network is 7.75, which is close to the average degree of 8, used in the earlier SIR simulations.

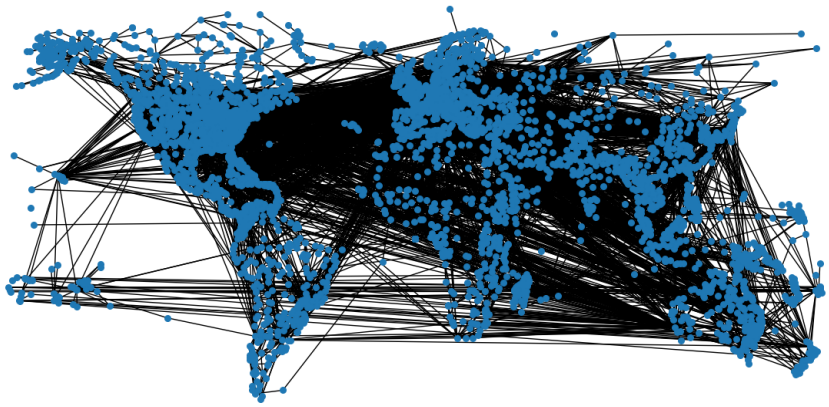

FIGURE 28: Visualisation of the international flight network. The nodes are airports, and the edges are flight connections.

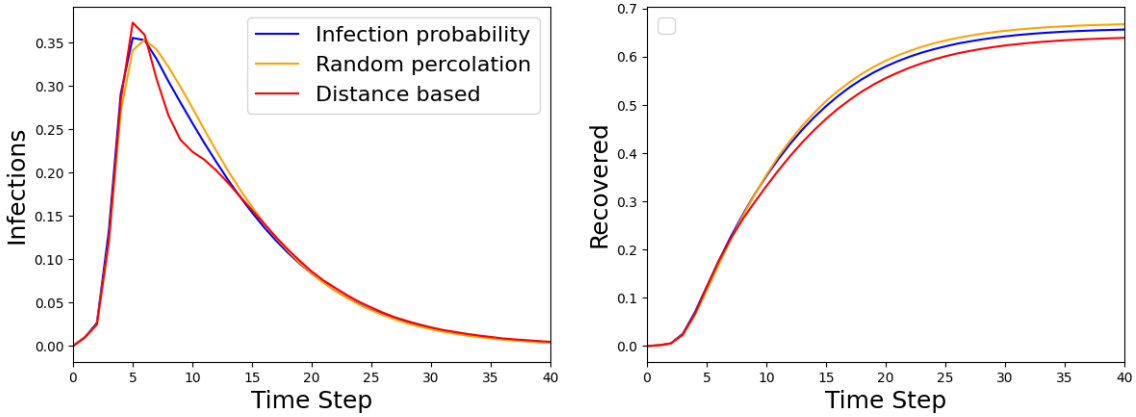

FIGURE 29: Infection (left) and Recovered (right) graphs of the four methods, on the airport network. Every line is the average of 200 simulations.

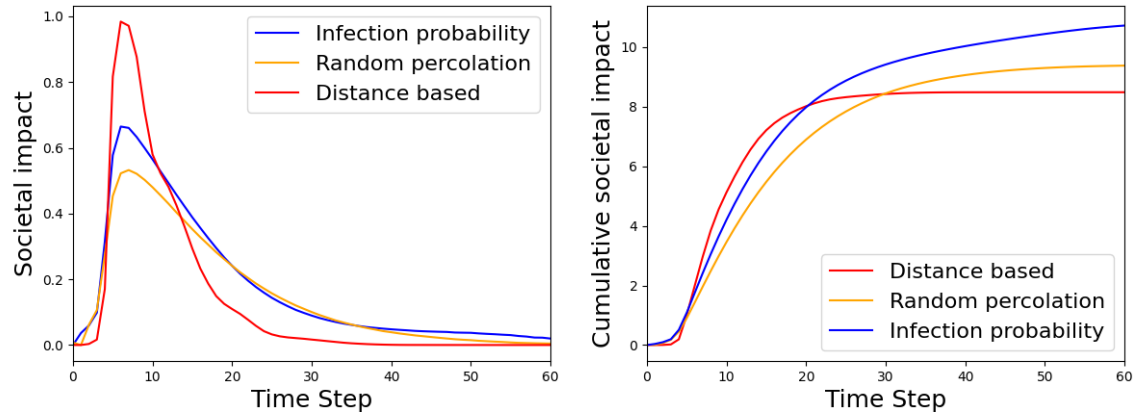

FIGURE 30: Societal impact (left) and cumulative societal impact (right) graphs of the four methods, on the airport network. Every line is the average of 200 simulations.

7 Discussion

In this section we will review the results from this thesis, and interpret their significance. We will compare the outcomes with the existing literature. Furthermore, we will go into the limitations of our models, which leads to possible improvements and further research recommendations.

7.1 Analysis of simulation results

In this thesis, we came up with four methods to model adaptive intervention strategies. In Section 6.3 we compared the four methods on the SIR, SITS and SIS models. On the SIR model, the distance based method most effectively reduced the peak, while the weight based method led to the lowest total number of infections. On the SITS model we saw similar behaviour, but the strict interventions of the distance based method led to more peaks and higher second peaks. On the SIS simulations, we saw that all the four methods converge to an equilibrium state. The distance based method takes multiple oscillations to get to the equilibrium, while the other methods get to the equilibrium in the first peak. While the SDP values where chosen such that the societal impact is nearly the same, the equilibrium of the weight based method lies notably lower than the equilibria of the other methods.

In Section 6.4 we saw that the local methods outperformed their global counterparts in every metric. With less societal impact they lead to lower and delayed peaks, and less total infections. This is a very interesting, but also explainable outcome. The local methods focus on decreasing the infectiousness or the network connectivity around the infections. Instead of deleting contacts between two healthy individuals, they only target individuals that observe a high prevalence in their social network. This means there is no unnecessary societal impact, which results in the local methods to be more effective with similar societal impact. This leads to the question if the effectiveness of local information models could be utilised in real life interventions strategies. Instead of global policies that are the same for everyone, policy makers could choose to let individuals decide their extent of social distancing, based on their locally observed prevalence. This however assumes that individuals have access to the information of who is contagious in their social network. Also, such policies might be regarded as vague and impractical, which could lead to low adherence to the policies. One could also view the effectiveness of the local methods in a different light. Even if the intervention strategies are the same for everyone, the adherence to the strategies might depend on local information. If an individual observes a lot of infections in their social network, they are more likely to adhere to intervention strategies. In this way, local information might be a useful tool to model human behaviour during epidemics.

In Section 6.5 we looked into the effects of information delay. On diseases with a high infection rate, delay has a large negative effect, since the disease has already extensively spread before the intervention strategies start. On diseases with a slower progression, delay has less impact. If the disease model also includes the possibility of reinfection, there might be simulations in which delay has a slight improvement over the situation with no delay. But, this was not shown to be significant.

In 6.6 we compared our adaptive models with threshold models. Interestingly, the adaptive methods do not significantly outperform the threshold models. This shows that

steady interventions after a certain threshold can be effective. This however, does not take into account the realism of the models. While the adaptive model accounts for the human behaviour to disease prevalence, the threshold model assumes full adherence to the interventions. Again, the weight based model was the most effective of the four interventions methods.

Over all the simulations, with multiple model setups, the weight based method showed to be the most effective method to mitigate viral spread, when the societal impact was equalized. Then the question arises, why the weight based method is the most effective and what we can learn from this. The weight based method is effective at targeting high degree nodes, so-called hubs. While the degree proportions stay the same, the hubs lose more connections. If hubs get infected, they might cause a significant acceleration of the disease spread with so-called super-spread events. The main takeaway from this for policy makers is that targetting the most connected individuals might be worth the effort.

7.2 Comparison with existing literature

While the scientific contributions to the field of epidemic modelling are vast, this is to our knowledge one of the first works that models disease spread on networks with interventions that depend on the prevalence of the disease. Since this is a new way of modelling, and the results are very dependent on the parameter choices, it is hard to directly compare outcomes from this model with existing literature.

7.3 Limitations and possible improvements

Since the spread of diseases is a very complex process, the models presented in this thesis are highly simplified. Social networks are much more complex than the networks that we used. People move, have evolving contacts, and the real social networks are of a different order of magnitude.

Section 6 gives a general overview of simulation results, but these results heavily depend on the choice of parameters. An already simplified model, like the one presented in this thesis, has numerous parameters. Extensively researching the influence of the different parameters and their interactions with each other, would cost a tremendous amount of time. Some choices of parameters in the results section have been supported by valid reasoning, while others have been chosen somewhat arbitrarily. Next to that, the results have not been validated by real world data. The results should be viewed in a modelling sense: they give information about what influence specific modelling choices have. They should not be regarded to be directly applicable for realistic disease representations.

Section 5 shows some theoretical results. While the outcomes are theoretically useful, they have not been tested empirically, due to time constraints. Next to this, the results have a lot of approximations, so they might not be very useful in practice. It would have been interesting to compare the theoretical SIS equilibria with the equilibria in simulations.

In our models we make the choice between the SIR, SIS and SITS model. While all of these models capture some specific essence of diseases, they are still simplifying. A real disease is continuous, while we use a discrete compartment model. People do not directly go from infected to recovered, this is a continuous process. To more realistically model diseases with compartments, we would need much more compartments. For example, the

Infected compartment could be split up in Mild, Medium, and Severe sub-compartments. While this would make the model more realistic, it is also harder to reflect on the outcomes of such models, because visualising a disease with much more compartments will be challenging. Another compartment that would be interesting to add is a Vaccinated compartment, since this adds another dynamic to the model. But again, this adds more complexity and parameters to the model, so it will be harder to analyse.

Another discretization is made with the time steps. To simulate the spread of the disease, we have chosen for a time discretization. Every time step, the statuses of the individuals are being updated. In real life this is also a continuous process. Instead of using time discretization, we could have chosen to use discrete-event simulations (DES). Here each event, for example an infection, occurs at a particular instant in time. In between consecutive events, no change in the system is assumed to occur, so the simulation time can directly jump to the time of the next event. This makes DES in general faster than using a time discretization. We however, chose to use time discretization for its simpler implementation.

While this thesis models the compliance to intervention strategies, we do not claim to have expert knowledge about human behaviour. In our model, the effectiveness or compliance to the interventions is directly linked to the disease prevalence. Of course, human behaviour during epidemics is much more intricate. The human behaviour is more linked to perceived risk than to the actual disease prevalence. Our model could be used as starting point for more specific studies to model human behaviour during epidemics.

7.4 Future research

This work lays a foundation for other works to build on. The framework for modelling adaptive intervention methods on networks has the potential to become an important part of epidemic modelling, but there is a lot for future work to do. The models could be made more complex and realistic by adding more compartments, and could be sped up by using discrete-event simulations. A faster model could be useful to do more simulations with different parameter settings. The choice of parameters could also be a good direction for future research. The results could be compared with real world data to find values, for example for SDP, that align with real epidemics. Next to this, the theoretical results on the SIS equilibria could be tested against simulation results.

Another interesting direction for future research is the combination of the adaptive model with the threshold model. The interventions would start after a certain threshold on the prevalence, but the strength of the interventions would then also depend on the prevalence. Next to this, we could also combine the distance or weight based model with the infection probability method. The distance based method would mimic the interventions that focus on long distance travelling, while the infection probability method mimics the interventions that focus on reducing infectiousness, such as hygiene.

8 Conclusion

Our research question was '*How do adaptive intervention strategies on geometric random graphs influence the spread of infectious diseases?*'. This thesis introduced four methods to model adaptive interventions that change based on the disease prevalence. The weight based method scales the weights of the GIRGs based on the disease prevalence. The distance based method deletes the longest edges. The infection probability based method does not change the network, but reduces the infectiousness. The random percolation method randomly deletes edges, and is used as benchmark to compare our strategies with. From the four methods investigated in this thesis, the weight based intervention method turned out to be the most effective in reducing the total number of infections for multiple model setups, such as SIR and SIS. Its effectiveness can be explained due to its focus on super spreaders. The distance based intervention method also showed its effectiveness, for example in reducing the peak infections. The distance based method was especially effective in combination with local information.

Next to the four intervention strategies, this thesis introduced local information. Instead of looking at the global prevalence, we investigated the effect of only looking at the infection status of neighbours. This thesis showed that local intervention strategies outperform their global counterparts by only targeting high-prevalence areas. Furthermore, we investigated the effect of information delay. In general, delay has a negative effect on the mitigation of viral diseases, especially when the disease has a high infection rate.

Lastly, it was shown that adaptive intervention strategies do not significantly outperform threshold methods, but the adaptive methods do capture human behaviour better than the threshold methods.

The key contribution from this thesis is that it develops a novel framework on integrating adaptive intervention strategies on networks into epidemic modelling. These adaptive methods can be used to add human behaviour to epidemic modelling, since this is currently an underdeveloped area. We hope that this thesis contributes to the modelling of epidemics, such that possible future policies can be more efficient and less disruptive.

References

[1] Air transportation networks. https://seeslab.info/downloads/air-transportation-networks/. Accessed: 2024-12-11.

[2] Emerging infectious diseases. https://www.hopkinsmedicine.org/health/conditions-and-diseases/emerging-infectious-diseases. Accessed: 2025-14-02.

[3] Had covid recently? here's what to know about how long immunity lasts, long covid, and more. https://www.aamc.org/news/had-covid-recently-here-s-what-know-about-how-long-immunity-lasts-long-covid-and-more. Accessed: 2025-28-01.

[4] What to expect while recovering from covid-19. https://www.bswhealth.com/blog/what-to-expect-while-recovering-from-covid-19. Accessed: 2025-14-02.

[5] Who covid-19 dashboard. https://data.who.int/dashboards/covid19/deaths. Accessed: 2024-10-12.

[6] Thomas Bläsius, Tobias Friedrich, Maximilian Katzmann, Ulrich Meyer, Manuel Penschuck, and Christopher Weyand. Efficiently generating geometric inhomogeneous and hyperbolic random graphs. *CoRR*, abs/1905.06706, 2019.

[7] B. Bollobás. A probabilistic proof of an asymptotic formula for the number of labelled regular graphs. *European Journal of Combinatorics*, 1980.

[8] Karl Bringmann, Ralph Keusch, and Johannes Lengler. Geometric inhomogeneous random graphs. *Theoretical Computer Science*, 760:35–54, 2019.

[9] Nuno Crokidakis. Covid-19 spreading in rio de janeiro, brazil: Do the policies of social isolation really work? *Chaos, Solitons Fractals*, 136:109930, 2020.

[10] Silvio L.T. de Souza, Antonio M. Batista, Iberê L. Caldas, Kelly C. Iarosz, and José D. Szezech Jr. Dynamics of epidemics: Impact of easing restrictions and control of infection spread. *Chaos, Solitons Fractals*, 142:110431, 2021.

[11] Joshua M. Epstein, Jon Parker, Derek Cummings, and Ross A. Hammond. Coupled contagion dynamics of fear and disease: Mathematical and computational explorations. *PLOS ONE*, 3:1–11, 12 2008.

[12] A. Erdős, P.; Rényi. On random graphs. *Publicationes Mathematicae*, 1959.

[13] Eli P. Fenichel, Carlos Castillo-Chavez, M. G. Ceddia, Gerardo Chowell, Paula A. Gonzalez Parra, Graham J. Hickling, Garth Holloway, Richard Horan, Benjamin Morin, Charles Perrings, Michael Springborn, Leticia Velazquez, and Cristina Villalobos. Adaptive human behavior in epidemiological models. *Proceedings of the National Academy of Sciences*, 108(15):6306–6311, 2011.

[14] Joost Jorritsma, Tim Hulshof, and Júlia Komjáthy. Not all interventions are equal for the height of the second peak. *Chaos, Solitons Fractals*, 139:109965, 2020.

[15] W. O. Kermack and A. G. McKendrick. A contribution to the mathematical theory of epidemics. *R. Soc. Lond. A115700–721*, 1927.

[16] Vitor M. Marquioni and Marcus A.M. de Aguiar. Quantifying the effects of quarantine using an ibm seir model on scalefree networks. *Chaos, Solitons Fractals*, 138:109999, 2020.

[17] Angélica S. Mata and Stela M. P. Dourado. Mathematical modeling applied to epidemics: an overview. *São Paulo Journal of Mathematical Sciences*, 15, 2021.

[18] Riccardo Michielan, Nelly Litvak, and Clara Stegehuis. Detecting hyperbolic geometry in networks: Why triangles are not enough. *Phys. Rev. E*, 106:054303, Nov 2022.

[19] Akhil Panicker and V. Sasidevan. Social adaptive behavior and oscillatory prevalence in an epidemic model on evolving random geometric graphs. *Chaos, Solitons Fractals*, 178:114407, 2024.

[20] Chadi M. Saad-Roy and Arne Traulsen. Dynamics in a behavioral–epidemiological model for individual adherence to a nonpharmaceutical intervention. *Proceedings of the National Academy of Sciences*, 120(44):e2311584120, 2023.

[21] David-Rus D. Schälte Y. et al. Syga, S. Inferring the effect of interventions on covid-19 transmission networks. *Sci Rep 11, 21913*, 2021.

[22] Yifokire Tefera, Abera Kumie, Damen Hailemariam, Samson Wakuma, Teferi Abegaz, Mulugeta Tamire, and Shibabaw Yirsaw. Impact of covid -19 incidence rate and government-initiated risk communication measures on individual's npi practices. *PLOS ONE*, 19:1–16, 03 2024.